Follow-The-Leader Mechanisms in Medical Devices

A Review on Scientific and Patent Literature

Culmone, Costanza; Yikilmaz, Semih Fatih; Trauzettel, Fabian; Breedveld, Paul

DOI
10.1109/RBME.2021.3113395

Publication date
2023

Document Version
Final published version

Published in
IEEE Reviews in Biomedical Engineering

Follow-The-Leader Mechanisms in Medical Devices: A Review on Scientific and Patent Literature

Costanza Culmone, Fatih S. Yikilmaz, Fabian Trauzettel, and Paul Breedveld

(Methodological Review)

***Abstract*—Conventional medical instruments are not capable of passing through tortuous anatomy as required for natural orifice transluminal endoscopic surgery due to their rigid shaft designs. Nevertheless, developments in minimally invasive surgery are pushing medical devices to become more dexterous. Amongst devices with controllable flexibility, so-called Follow-The-Leader (FTL) devices possess motion capabilities to pass through confined spaces without interacting with anatomical structures. The goal of this literature study is to provide a comprehensive overview of medical devices with FTL motion. A scientific and patent literature search was performed in five databases (Scopus, PubMed, Web of Science, IEEExplore, Espacenet). Keywords were used to isolate FTL behavior in devices with medical applications. Ultimately, 35 unique devices were reviewed and categorized. Devices were allocated according to their design strategies to obtain the three fundamental sub-functions of FTL motion: *steering*, (controlling the leader/end-effector orientation), *propagation*, (advancing the device along a specific path), and *conservation* (memorizing the shape of the path taken by the device). A comparative analysis of the devices was carried out, showing the commonly used design choices for each sub-function and the different combinations. The advantages and disadvantages of the design aspects and an overview of their performance were provided. Devices that were initially assessed as ineligible were considered in a possible medical context or presented with FTL potential, broadening the classification. This review could aid in the development of a new generation of FTL devices by providing a comprehensive overview of the current solutions and stimulating the search for new ones.**

***Index Terms*—Minimally invasive surgery, path-following, shape memory systems, snake robots, surgical robotics.**

Manuscript received 25 February 2021; revised 20 July 2021; accepted 30 August 2021. Date of publication 20 September 2021; date of current version 6 January 2023. This work was supported in part by the research program Bio-Inspired Maneuverable Dendritic Devices for Minimally Invasive Surgery under Project 12137, in part by The Netherlands Organization for Scientific Research (NWO), and in part by the European Union's Horizon 2020 Research and Innovation Programme under the Marie Sklodowska-Curie Grant Agreement 813782.

The authors are with the Department of Biomechanical Engineering, Delft University of Technology, 2628 CD Delft, The Netherlands (e-mail: c.culmone@tudelft.nl; f.s.yikilmaz@student.tudelft.nl; f.trauzettel@tudelft.nl; p.breedveld@tudelft.nl).

Digital Object Identifier 10.1109/RBME.2021.3113395

I. Introduction

IN THE last decades, minimally invasive surgery (MIS) has shown many benefits over open surgery, due to a reduction in the size of incisions made by the surgeon [1]–[3]. Ultimately, MIS leads to less scar tissue, bleeding, infections, and hospital time [4]–[6]. Conventional MIS involves the use of rigid, slender instruments inserted into the body via trocars. In some cases, such as in laparoscopic surgery, the surgeon's maneuverability and vision can be improved by creating an open space by inflating the body with carbon dioxide. However, this technique cannot always be used. In some procedures, natural anatomic pathways such as blood vessels can be used to reach the target area using passively flexible instruments, e.g., flexible endoscopes or catheters. However, in situations in which natural pathways cannot be used to reach the target area, external guidance, and support of the instruments is necessary. This issue becomes fundamental in natural orifice transluminal endoscopic surgery (NOTES), in which surgeons use the mouth, nostrils, rectum, and other natural orifices to enter the human body [7]–[10]. In these scenarios, rigid or passively flexible instruments are limited in their dexterity, which negatively impacts the positive outcome of the procedure [11]. It is therefore important to design medical devices that have high dexterity and additional degrees of freedom (DOF) to reach targets in confined anatomical structures. Features like controllable flexibility have been used in the design of many medical devices [12], [13]. Controllable flexibility allows for surgical instruments to access target locations in a flexible state while providing rigid support during the procedure phase. Another important feature is the device control strategy that is the way to navigate the instrument into the body and plan the pathway. One of the most applied control strategies is the so-called Follow-The-Leader (FTL) motion, first proposed by Choset and Henning in snake-like hyper redundant robots [14]. These robots possess bio-inspired serpentine locomotion in which the body of the robot follows its tip. This motion allows the device to reach a target in a confined space from one entry point without relying on reaction forces from the environment. A definition of FTL motion for a medical instrument is given by Burgner-Kahrs *et al.* [15], stating that these devices must "*operate in a so-called follow-the-leader manner where their body conforms approximately to the path taken by their*

end-effector without relying on anatomical interaction forces." This behavior makes it possible to avoid obstacles at all times during advancement towards a target or retraction from a target, without applying significant force to any anatomy.

The goal of this study is to provide a comprehensive overview of methods used to achieve FTL motion in medical devices from both scientific and patent literature. For inclusion in this study, the device should be mechanically described and, a physical or a virtual prototype should be presented. Moreover, the device should memorize and propagate along the path taken by the end-effector to comply with the FTL motion. The devices found in the literature are classified based on the mechanical aspects providing their FTL motion.

II. Literature Search Methods

A. Scientific Literature Search

The scientific literature search was conducted using the Scopus, PubMed, Web of Science, and IEEExplore databases. Because the goal was to provide a comprehensive overview of medical devices that have been designed to have FTL motion ability, the query was organized in three main aspects named: *behavior*, *object*, and *application*. All of these aspects had to be present in the found papers to merit their inclusion in this study. The behavior terms of the query specify the nature of the devices' motion. Here, *follow the leader∗, shape memor∗, path follow∗, snake-like,* and *serpentine* were used as search terms to capture this aspect. In the object category, *device∗, instrument∗, catheter∗,* and *manipulator∗* were specified to define the type of device sought, in this case, any type of medical device. Finally, the application category specified the medical application in which the sought devices could be used; *∗medic∗, surg∗, interven∗, ∗scop∗, inspec∗, diagnos∗, treat∗,* and *therap∗* were specified for this term. The query was restricted to title, abstract, and keywords because these areas contain the essence of the article.

The query was formulated as follows: ("follow the leader∗" OR "shape memor∗" OR "path follow∗" OR "snake like" OR "serpentine") AND (catheter∗ OR instrument∗ OR device∗ OR manipulator) AND (∗medic∗ OR surg∗ OR interven∗ OR ∗scop∗ OR inspec∗ OR diagnos∗ OR treat∗ OR therap∗). The search was limited to English written documents only, and no time limitations were given. The query was aimed at isolating results about devices that have an FTL mechanism and are used in medical applications. The overlapping documents among different databases were filtered out. The query was discussed and formulated by all the authors of this review. The appearance of each word used in the query was further checked in the title, abstract, and keywords to evaluate its relevance for the search.

B. Patent Literature Search

The patent literature search was conducted using the Espacenet database. The query was limited to search within classification A61: *Medical or veterinary science; hygiene*, and further limited to titles and abstracts ("ta"). The query was expressed as follows: *(ta = "follow the leader" OR ta = "path follow∗" OR ta = "snake like" OR ta = "serpentine∗") AND (ta any "catheter∗" OR ta any "instrument∗" OR ta any "device∗" OR ta any "manipulator∗") AND cpc = "A61"*. Because the search was already within the medical classification A61, the application category became redundant and was omitted. The term *shape memor∗* was also omitted from this query, as even though within the context of FTL motion, it refers to the ability of a device to remember its physical shape, most often the term is used in materials science, leading to too many irrelevant results. Finally, the results were filtered to show English results only.

C. Eligibility Conditions

In order to be deemed eligible for inclusion, an item of literature had to demonstrate a clear medical application, have met all of the conditions for FTL motion set out by Burgner-Kahrs *et al.* [15] in Section I, which means be able to memorize and propagate the path taken by the end-effector, and have disclosed the mechanical design of the presented robot, either as a physical prototype or virtual model. Papers containing only algorithms or clinical trials of FTL devices without mechanical background information were not included.

In many cases, FTL systems are not designed for medical purposes but rather for search and rescue or inspection in an industrial setting [16], [17]. These systems face fundamentally different design requirements as compared to medical robots, often directly using their environment to provide the reaction forces necessary for movement, a strategy that is undesirable in the medical field due to the risk of tissue damage. This results in methods of locomotion that are significantly different from those designed to interact with human tissue (e.g., wheels [18], continuous tracks [19], or legs [20]). Finally, these robots are much larger than their medical counterparts [21], [22], which are designed to operate in confined spaces at comparatively small scales while maintaining biocompatibility and sterility and interacting with human tissue. Solutions for search and rescue or industrial inspections were therefore not included in the study.

The performance of the presented devices did not affect their selection. For example, some devices cannot carry their weight and therefore need a surface to operate on [23] or need to be operated hanging down [24]. In these cases, if the FTL motion is still present and independent from the environment in at least one plane, the paper was included.

III. Results

A. Literature Search Results

The literature search yielded 6638 scientific papers and 158 patents. Of the located pieces of scientific literature, 3119 results were located using Scopus, 2376 were sourced using the Web of Science database, 876 results were found on PubMed, and 267 on IEEExplore Fig 1. Duplicates were removed by comparing titles with a Matlab script that selected 3997 individual scientific papers (last update: June 2021). The titles and abstracts of the found papers and patents were manually checked to exclude documents dealing with topics different from FTL motion in

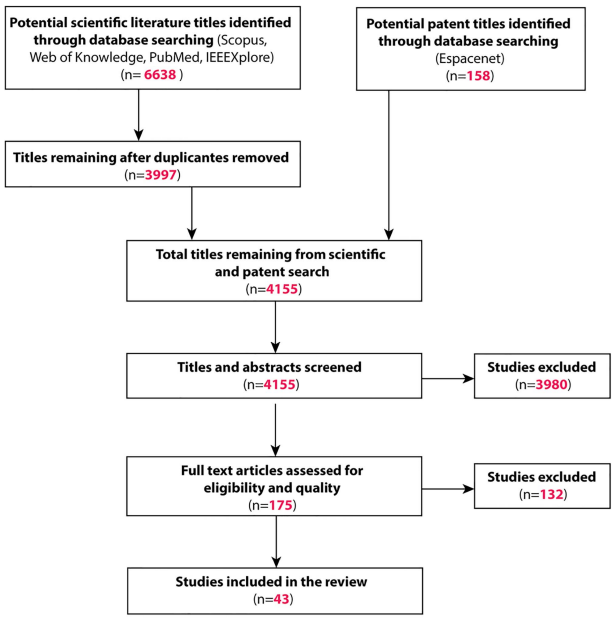

Fig. 1. Four-phases flow diagram for the scientific and patent literature.

medical devices. This selection resulted in 175 potentially relevant scientific papers and 21 patents. The full texts of these documents were then read and examined based on the eligibility conditions by the authors. The references were also checked to find other relevant papers or patents. Finally, 43 documents were selected from the scientific and patent literature, covering in total 35 different FTL devices. The final results were discussed and checked by all the authors.

B. General Categorization

In order to categorize the devices found in the literature, the concept of FTL motion was divided into three sub-functions: *steering*, *propagation*, and *conservation*, as shown in Fig. 2. The principle is that any device capable of FTL motion must possess all three sub-functions. An FTL system must be able to:

1) Steer the leader/end-effector to the desired orientation.
2) Propagate along a specific path towards a target.
3) Conserve the shape of the path taken by the leader/end-effector.

Each sub-function was further divided into the *type* of solution to achieve the sub-function, Fig. 2. Each type of solution was then analyzed considering the *method* to generate forces for the given sub-function. Since patents often intentionally cover a variety of suitable actuation methods, the most emphasized method was assumed for the classification. Throughout this review, the word "proximal" is used to indicate the shaft segments that are closest to the operator or handle of the device, whereas "distal" is used for the segments that are close to the end-effector of the device.

C. Steering of the Device

For FTL devices, steering the device essentially means manipulating the orientation of the leader/end-effector. The steering classification concerns the location of the steering actuator(s) - either inside or outside the body. *Steering/Inside the body* indicates that the actuation unit is embedded in the part of the device that must be inserted into the body of the patient (e.g., the shaft or the steerable segments). *Steering/Outside the body* means that the actuation systems of the robot are not inserted into the body of the patient, but remain in a module of the robot (e.g., handle or controller) that is kept outside of the patient.

The steering motion is generated by forces that actuate the segment leader/end-effector. The found methods by which these forces are generated in steering both inside and outside the body have been subdivided into six groups:

a) motor torque or force
b) thermal deformation force
c) elastic relaxation force
d) electromagnetic (EM) force
e) cable tension force
f) hydraulic force

In these groups the leader segment changes orientation because (a) a torque is applied to its joint by a motor; (b) it is attached to wires that change their shape with heat; (c) it wants to assume the orientation with the lowest potential energy; (d) it is attracted by an electromagnetic force pivoting it in a certain direction; (e) it is pulled by a cable that bends or pivots the segment towards a certain direction; f) it is filled with a pressurized liquid.

1) Steering/Inside Body: This group consists of devices that have actuators embedded within the parts that enter the body of the patient [23], [25]–[31]. Most of these devices have segments with embedded motors that control the joint rotation of each segment individually by applying torque [27], [28], [31]. A unique case is a device proposed by Chen *et al.*, shown in Fig. 3(a) [23]. This particular device uses motors embedded in the segments to reel in cables and bend the segments with cable tension. Systems that steer by means of shape memory alloy (SMA) wires, also referred to as SMA actuators [32], [33], are also considered to have an actuation inside the body of the patient [25], [26]. Actuation by SMA wires is carried out using a material phase change. By changing the temperature of SMA wires, the atomic arrangement of the material changes [34], reshaping the wire. If these wires are attached to segments of the FTL device, their deformation can re-orient the segment. If the temperature is precisely and actively controlled, the deformation of the SMA wire can be regulated, making the steering (semi-) continuous (Fig. 3(b)) [26]. If the SMA wire is only set to achieve the threshold for total deformation, the segments have a binary control assuming only their extreme orientations when activated [25]. Note that in these devices, the temperature increases due to current flow through electrical resistance within the wires. One of the analyzed devices instead uses electromagnetic (EM) force to pivot the segment to its extremes in one DOF, obtaining binary steering for each segment, see Fig. 3(c) [29], [30]. The EM force is generated within the segments and is therefore categorized as an actuator inside the body.

2) Steering/Outside Body: This group consists of devices that have actuators in the proximal handle or controller, external to the parts that enter the body of the patient. For most of these

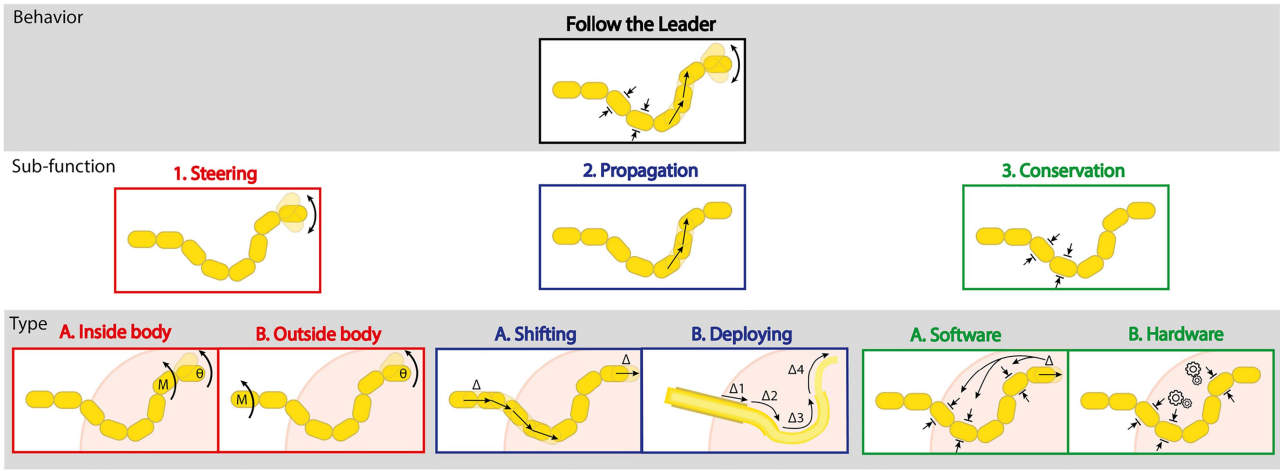

Fig. 2. Schematic representation of follow-the-leader motion divided into three sub-functions. 1. Steering, 2. Propagation, 3. Conservation. Each sub-function is further analyzed considering the actuator location, propagation manner, and constraint type, respectively.

devices, the steering is achieved using cables [24], [35]–[58]. Pulling or releasing the cables changes the curvature of the device's segments. Tensile force on the cables can be applied by actuators located outside the body, e.g., electromotors [24], [35]–[38], [40]–[49], [51]–[56], [59] or manually [39], [50], [57], [58]. The number of DOF achievable by any given steerable segment is dependent on the number of cables controlling it; two cables result in one DOF, whereas three or four cables result in bending in two DOF. A common arrangement for these devices consists of rigid spacer disks that guide the cables along the shaft of the device, with these disks attached to [35] or arranged around one compliant element [41], [42], [46], running the entire length of the shaft (Fig. 3(d)). As this design is analogous to a vertebral column, the central element is often referred to as the "backbone" [60]. In devices with multiple steerable segments, the cables controlling a given segment simply pass through the disks of the segments they are not intended to control and are anchored only to the segment they control. By pulling at the steering cables a local bending torque, which directly relates to the length of the moment arm relative to their backbone, is applied, causing the segment to steer. Cables can also be substituted by pressurized liquids. The combination of more than two jets bends the segments in two DOF [61], Fig 3(e).

Elastic relaxation forces are used for steering devices composed of pre-curved concentric tubes [62]–[69]. Pre-curved concentric tube devices consist of plastically bent tubes aligned concentrically, Fig. 3(f). Here, steering is essentially the result of the elastic interaction of the tubes. The tubes naturally want to bend in a certain direction, therefore applying elastic relaxation forces. By rotating and translating the tubes with respect to each other, the pre-curved sections will change their orientation [62]. The rotations and translations of the tubes are achieved using actuators outside the body. As the motion comes from the internal elastic forces of the tubes, these devices do not need cable guiding disks or the creation of space between a backbone and a tendon to allow moment arms to apply forces [70]. These types of systems are also called invertebrate robots due to the lack of a backbone compared to tendon-driven devices. They are quite popular in the field of medical instruments because their working principle allows the construction of very thin devices [71], [72] compared to cable-driven devices. In cable-driven devices, the bending torque depends on the length of the moment arm relative to the backbone, requiring a certain thickness for functioning.

D. Propagation of the Device

The propagation classification concerns the advancement method only of the shaft of the device. The propagation of an FTL device is essentially the movement of the device shaft along a path towards a target. The device shaft can either advance in a shifting manner or a deploying manner. *Shifting propagation*, as defined by Ikuta *et al.*, means that the entire device shaft is part of the advancing movement [26]. All segments will advance the same distance simultaneously. *Deploying propagation* means that a distal segment of the shaft can advance while its proximal segments remain stationary.

The methods found for generating the forces to provide shifting or deploying propagating motion have been subdivided into two groups:

a) motor force (e.g., rack and pinion or lead screw spindle)
b) manual force (e.g., surgical handle or manual insertion)

1) Shifting Propagation: This group consists of devices that propagate by advancing all segments of the shaft simultaneously. Most of the found devices advance with an electric motor to continuously have precise control and information of the displacement [24], [26], [27], [29], [30], [37], [38], [40], [45], [47]–[49], [52], [55], [56], [61], Fig. 4(a). Conversely, some prototypes do not have real-time information on device advancement, thus they are programmed to steer segments on time for a constant advancement speed [23], [25], [31]. Other devices are designed for manual insertion and have other aids to account for the insertion depth [28], [50], [57], [58]. An example of the latter is the semi-automatic snake robot for NOTES shown

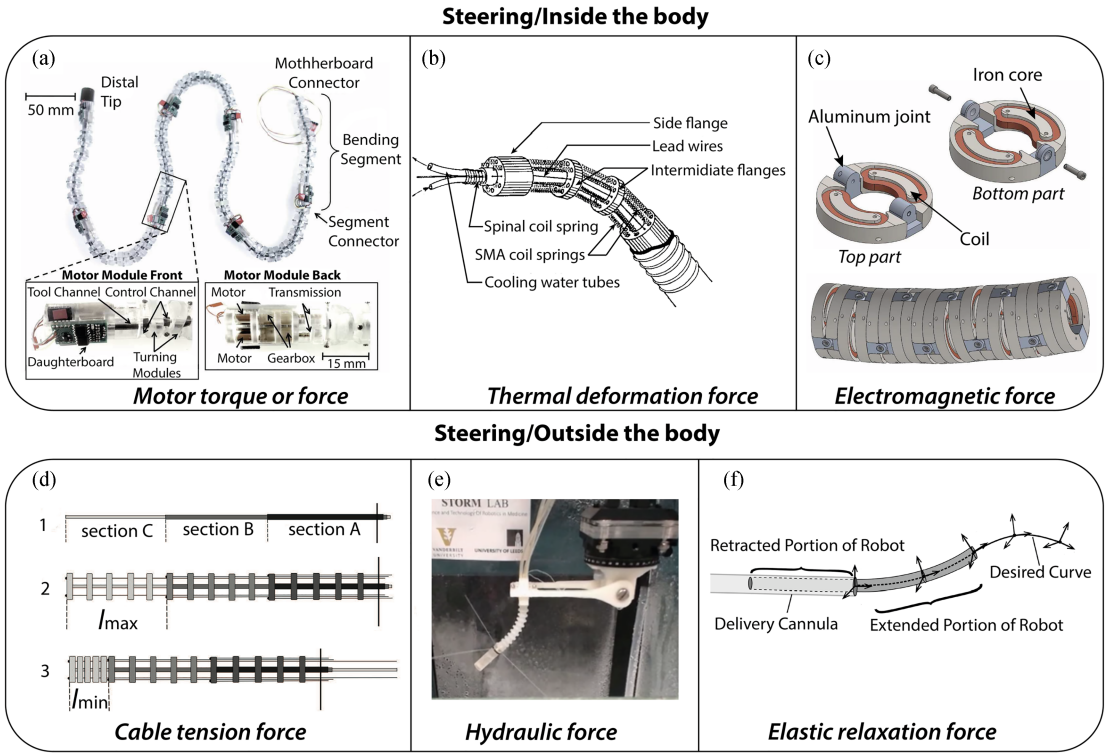

Fig. 3. Examples of actuators inside and outside the body of a Follow-The-Leader (FTL) devices. (a) Continuum robot endoscope. The motors in the motor modules reel in the cables attached to the segment connectors to articulate the segments [23] (© [2014] IEEE). (b) Inside structure of an active endoscope controlled by SMA actuators. The SMA coils contract when heated up and relax when cooled down with cooling water. The SMA coils are attached to flanges that bend by activating the SMA actuators [26] (© [1988] IEEE). (c) CAD model of a hyper-redundant FTL system. Each segment is composed of two grey rings. The grey rings are attached to each other using aluminum joints. The coil (red) around the iron core generates a magnetic field if current runs through it. Depending on the current direction, the rings swivel relative to their neighbors because of electromagnetic attraction/repulsion. Adapted from [29], [30] (© [2015] IEEE). (d) Two-dimensional schematic view of an extendable, tendon-driven continuum robot, adapted from [46]. The robot body is divided into three sections, with distal section C at the top and proximal section A at the bottom and connected to a control unit (not shown). Each section A-C contains five disks loosely placed around a backbone tube in the middle, with the tube connected to the top disc. The three backbone tubes of sections A-C fit concentrically into one another and are individually retractable. The top disc of section C connects to three tendons that pass freely through the system to the control unit. Similarly, the top disc of section B connects to three other tendons, and the top disc of section C connects to a third set of three tendons. In total, nine tendons are controlled by the control unit, as well as the length of the telescopic backbone tubes. If the distal tube is retracted, section C collapses. Permanent magnets are oriented in a repelling sequence to ensure equal distance when the concentric backbones are deployed. (e) Hydraulic actuated device. The pressurized water in the main body bends the device in different directions, adapted from [61]. (f) Concentric tube device. The tubes bend in the direction of the least internal tension. Operating this precisely results in steering [62] (© [2015] IEEE).

in Fig. 4(b). The device is inserted manually, and its insertion depth is tracked by a trans-anal endoscopic microsurgery (TEM) trocar equipped with hall-effect sensors [28]. Another manually operated device that does not need an external tracer module is the hyper-redundant surgical instrument shown in Fig. 4(c). The manually actuated passive rack and pinion mechanism advances the device by turning a crank, which creates a direct kinematic relation between the crank rotation and the forward motion of the device [57].

2) Deploying Propagation: This group consists of devices that propagate by advancing the relative distal segments of the shaft while the relative proximal segments of the device remain stationary, e.g., in Fig. 4(d), tubes 3 and 2 remain stationary while tube 1 advances. Since concentric tube systems propagate a tube while another remains stationary, these systems usually advance in a deploying manner by means of linear motor force. Three different types of concentric mechanisms have been found in the literature: pre-curved concentric tubes, steerable concentric devices, and alternating devices. *Pre-curved concentric tubes* [62]–[69], often referred to as telescoping mechanisms [66], slide concentrically using a linear motor force, see Fig. 4(d). *Steerable concentric devices* [35], [39], [41], [42], [46], [51], [59] use the same deployment mechanism, but since this devices are not pre-curved, an additional force is required to actively steer the tubes. A particular type of such a concentric mechanism is based on spacer disks that cannot be fixed to the backbone since the backbone extends. To keep the equal distribution of disks along the backbone, the loose disks contain mutually repelling permanent magnets. This means that the individual disks in the mechanism behave as separated by a spring, but unlike a spring, which has a minimum compressed length, the magnetic field can be compressed until there is no space between the magnets [35], see Fig. 4(e). The third type of concentric mechanism is the so-called *alternating devices* that switch the stationary part of the system [36], [43], [53], [54]. Instead of having multiple concentric tubes telescopically advancing one

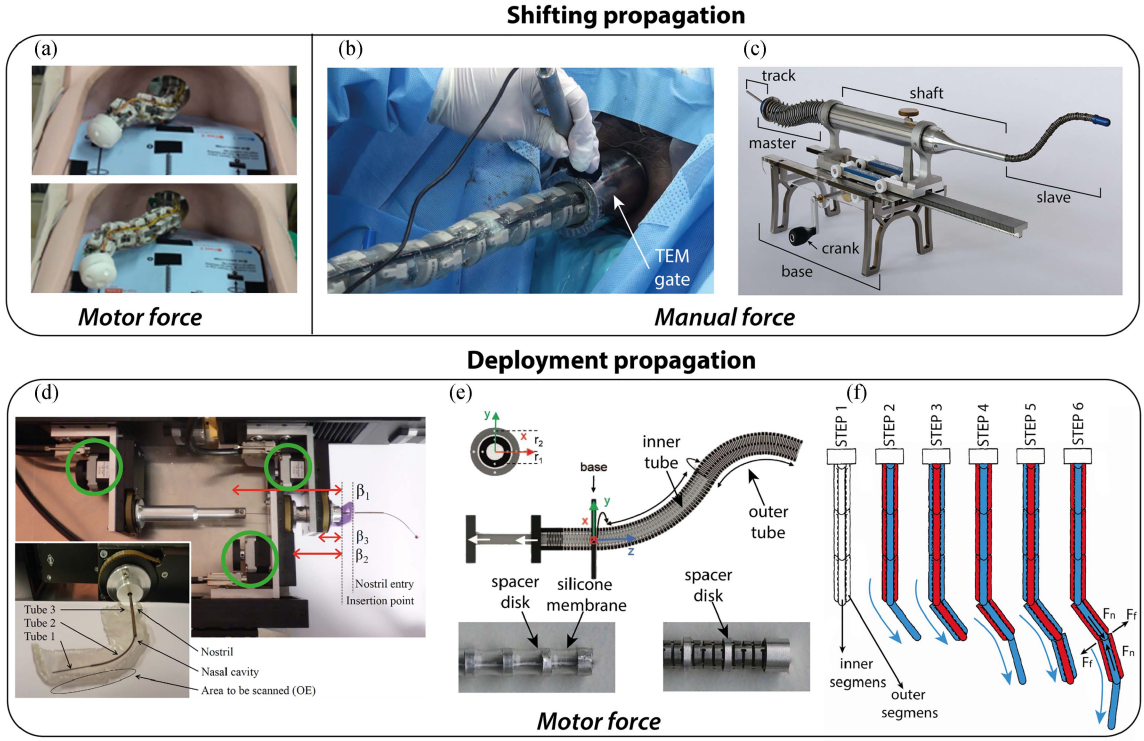

Fig. 4. Examples of Follow-The-Leader (FTL) devices with shifting or deploying propagation. (a) Example of shifting propagation in which all segments are independently controlled by dedicated motors on the external control unit. For the advancing motion, an additional motor moves the whole system, adapted from [37]. (b) Snake robotic colonoscope design concept named "hold the snake". The trans-anal endoscopic microsurgery (TEM) gate is placed in the patient's anus, and the robot is inserted through the TEM gate manually by a medical staff member. Electric motors embedded into the shaft segments control the steering and memorize the shape [28]. (c) MemoFlex hyper-redundant mechanical surgical FTL instrument, adapted from [57]. The crank drives a rack and pinion construction that translates the track – a pre-bent stainless-steel rod that defines the 3D path to be followed. During the forward motion of the instrument, the track moves through the master module in the direction of the shaft. The master module follows the shape of the moving track and is connected via cables to the slave module that copies the shape of the master. As the track moves through the master, the slave follows the shape of the track and thereby displays FTL motion over the fixed shape of the track. (d) Example of a concentric tube device designed for optical biopsy applications driven by stepper motors (encircled in green) [65] (© [2017] IEEE). (e) Tendon-driven continuum robot with an inner tube placed inside an outer tube. The spacer disks and silicone membrane provide a smooth concentric sliding motion, adapted from [35] (© [2017] IEEE). (f) Highly Articulated Robotic Probe (HARP). The inner and the outer tube alternate their stiffness during propagation: flexible while advancing (blue), stiff when stationary (red). Cables run through the segments of the inner and outer tubes. Tensioning the cables compresses the segments and generates normal forces (Fn) at their contact surfaces, thus locking the shape. The friction forces (Ff) between the contact surfaces of the segments keep the configuration locked, adapted from [43].

after another, these systems only have two concentric parts that switch in propagation; when the inner segments advance, the outer segments are stationary and vice versa, making it a deploying propagation. An example of this is shown in Fig. 4(f). As an alternative to this concentric version, the two alternating shafts can also be aligned parallel to each other [44].

E. Shape Conservation of the Device

Conserving the shape of an FTL device means assuming the shape of the path taken by the leader/end-effector during the entire propagation and memorize it. This means that the advancing segments of the device are essentially constrained in their movement. The constraint can be applied through the software or the hardware of the device. A *software constraint* means that the movement of the segment is determined by a computerized controller that maintains the configuration of the shaft of the device. Without a controlled actuation, this segment would be physically free to reconfigure. In practice, this implies that there is no dedicated mechanism other than the actuation system used for steering, which can preserve the global shape and pose of the shaft. In other words, the shape constraint is virtual, existing only in the control software of the device. Conversely, a *hardware constraint* means that a physical mechanism determines the movement of the segment. Note that the mechanism could still be activated using a controller, but the constraint on the movement of the segment is physical. The physical constraint can be applied in the handle or the shaft of the device. Naturally, the constraint type is closely related to the advancement method, as the shape is often conserved by the method of propagating.

1) Software Constraint: This group consists of devices that maintain their shape using a software constraint, where advancing segments have a virtually assigned direction. For this group, the shape is held by maintaining the position of the steering actuation. In devices with electric motors, the shape taken by the segment is held by holding the torque at each joint [27], [28], [31] (Fig. 5(a)). In devices with cables, the

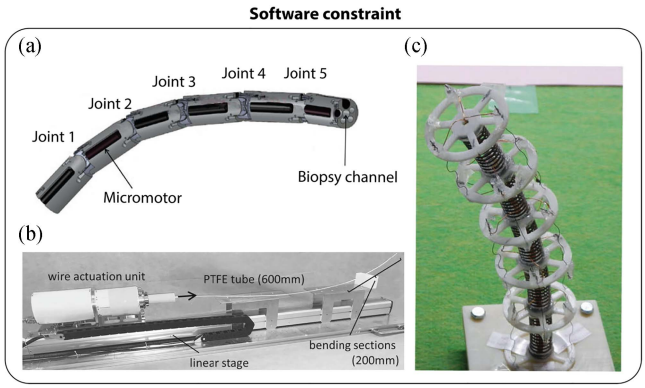

Fig. 5. Examples of software constraints. (a) Motor-based articulated robot. Each DOF is controlled by a motor placed directly into the steerable shaft. The shape is conserved holding the torque. Adapted from [27] (© [2013] IEEE). (b) Cable-driven catheter for transbronchial biopsy. The catheter uses a cable-driven push/pull mechanism to control the three steerable segments. The user uses a joystick to actively steer the end-effector and follow the path [55]. (c) Manipulator based on SMA actuators. Each segment is controlled by three SMA actuators. The orientation of the segment is obtained by heating up the SMA wires, adapted from [25].

position taken by the segments is kept by holding the tension on each segment [23], [24], [37], [38], [40], [45], [47]–[49], [52], [55], [56], and in devices with hydraulic actuation by holding the pressure [61] see Fig. 5(b). Devices with SMA actuators hold the shape by maintaining the right temperature for each segment [25], [26] (Fig. 5(c)), whereas devices with electro-magnets conserve their shape by maintaining the magnetic force [29], [30], Fig. 3(c). When propagating, the segments change their orientation to compensate for the change in configuration due to the device translation. This behavior can be achieved with inverse kinematics where the device configuration becomes the input for the computerized actuation and/or path planning algorithms that may use cost-functions to minimize the configuration perturbation.

2) Hardware Constraint: This group consists of devices where the shaft segments are physically constrained to advance only in the desired direction by a mechanism inside the shaft or the handle of the device. The found methods that generate the forces for shape conservation in devices based on hardware constraints can be subdivided into four groups:

a) *steering actuation force*
b) *friction force*
c) *interlocking geometry force*
d) *elastic interaction force*

where the shape of the device is maintained by (a) holding the actuation of the steering mechanisms (e.g., by applying torque or maintaining cable tension), (b) using friction forces in the shaft to prevent segment motion, (c) using interlocking structures in the shaft to prevent segment motion, or (d) leveraging the superposition of elastic interaction forces seeking minimum potential energy.

Most devices leveraging deploying propagation depend on advancing individual segments of the shaft in a particular sequence for the shape conservation method to work. These devices are classified as having a hardware constraint given by steering actuation forces [35], [41], [42], [46], [51], [59]. An example is shown in Fig. 6(a). The proximal segments of the device are advanced first and are steered along the desired path. Once the endpoint of its insertion movement has been reached, the segment stops moving and holds its shape. Thereby, it acts as a guide for a distal, concentrically aligned segment that begins a movement physically constrained to the path taken by the now stationary proximal segment. Since the leader segment is concentrically guided by its proximal follower segments, the device shape always conforms to the path taken by the leader.

The hardware constraint in pre-curved concentric tube devices is given by the elastic relaxation forces of the concentric tubes. If the (stationary) proximal tube has a strongly dominant stiffness relative to the (propagating) distal tube, the (stationary) proximal tube is considered to be a hardware constraint for the (propagating) distal tube [63]. However, if the tubes have similar stiffnesses, the device shape is determined by the superposition of the tube shapes [62], [64]–[69]. This means that the tubes have to re-orientate collectively to maintain the desired configuration being a hardware constraint for each other. The difference between these concentric tube mechanisms is schematically shown in Figs. 6(b)–(c). Due to the presence of pre-curved shapes, pre-curved concentric tube devices are limited in the paths they can follow [73].

As opposed to pre-curved concentric tube devices, in alternating devices, the concentric/parallel parts can be alternately locked and fixed in shape so that each of those two parts forms the stationary guide for the other as it propagates. This forms a hardware constraint for the concentric/parallel propagating part that slides along it. The alternating devices found in the literature use friction forces [36], [43], [44], [53], [54], or geometry locks [39] to hold the configuration of the stationary part. The friction force is achieved by compressing the segments with cable tension [43], [44], [53], [54], or by pinching the steering cables with piezo-electric deformation [36], Fig. 6(d). Geometry locking activated by cable tension or SMA actuators in an alternating device is proposed in the patent of Sadaat *et al.* [39]. Other interesting examples are the devices presented by Henselmans *et al.* [50], [57], [58], in which a geometry lock is used in the control handle outside the body to constrain the motion of the segments inside the body. Having the hardware constraint placed into the handle allows for larger space to design a dedicated locking mechanism that acts directly on the actuation of the segment. The locking mechanisms designed by Henselmans *et al.* contain either pre-curved rods [57] (Fig. 4(c)), pre-programmed physical tracks [50], or programmable physical tracks, such as the system shown in (Fig. 6(e)) [58].

IV. Discussion

A. Comparison of FTL Device Performance

1) Path Following Ability: One of the primary design goals of FTL medical devices is to allow better access to sites in tortuous anatomy whereas reducing the potential for patient injury due to contact between the shaft of the device and the

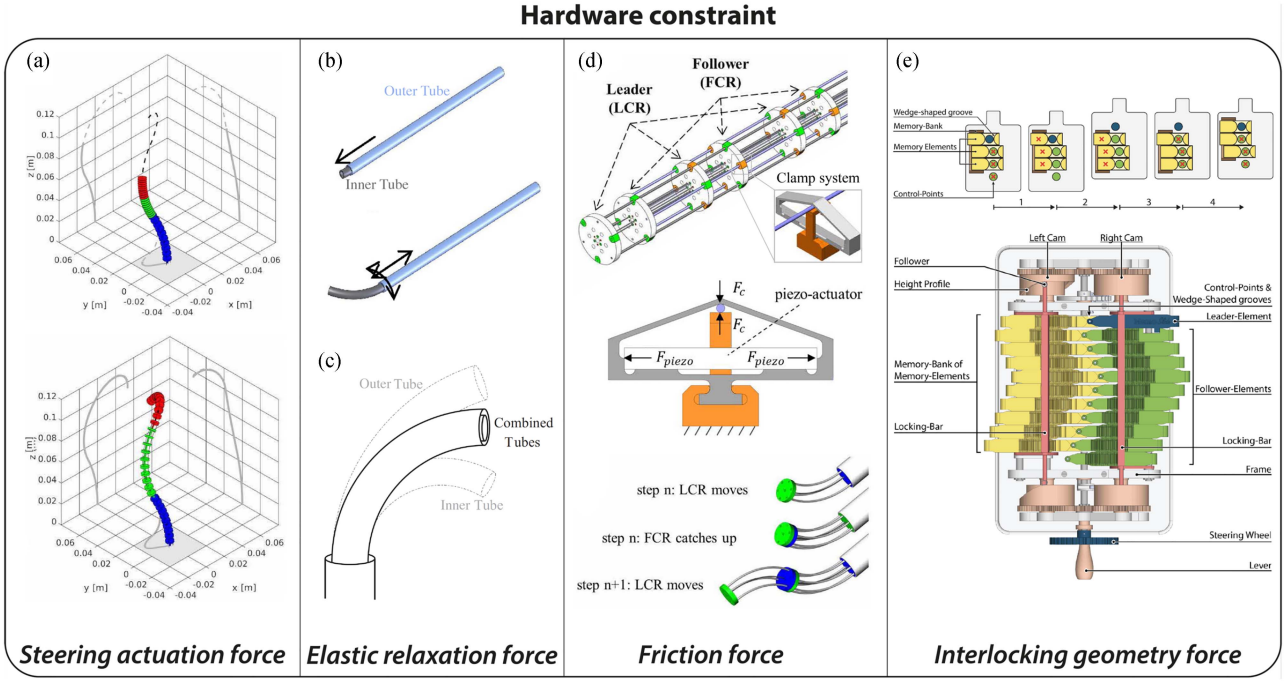

Fig. 6. Examples of hardware constraints. (a) FTL continuum robot. The segments are deployed in order from the most proximal (blue) to the middle (green) and, finally, the most distal segment (red). The shape of a relative proximal segment is held by the steering cables, while its relative distal segments advance concentrically through this fixed curve. Thus, the relative proximal segments form physical constraints to the advancement of the leader/end-effector towards the target [41] (© [2016] IEEE). (b) A pair of continuum concentric tubes with relative infinite stiffness of the outer tube (blue). When the inner tube (grey) is retracted, the outer tube dominates the stiffness and therefore the shape. When a portion of the inner tube slides out, the inner tube relaxes to its initial curvature [68] (© [2006] IEEE). (c) A pair of continuum concentric tubes with similar stiffness. A superposition of both inner and outer tubes with differently bent aligns the tubes in an intermediate position. The systems hold the configuration with elastic interaction forces, adapted from [114] (© [2006] IEEE). (d) The device consists of two identical tendon-driven continuum robots: the follower continuum robot (FCR) and the leader continuum robot (LCR). A clamp system, based on piezo-actuators, pinches the tendons, holding the configuration of the LCR and the FCR, alternately, adapted from [36]. (e) The MemoSlide programmable cam. The left figure shows the mechanism responsible for the MemoSlide shifting in which the main components of the mechanism are the leader element (blue), the follower control-points (green), and the memory elements (yellow). A red cross indicates when one of these components is geometrically locked. The right figure shows a top view of the proof-of-concept prototype. The memory and follower elements have teeth on the upper surface. These teeth interlock with the teeth on the bottom surface of the locking bars (red). When the lever is rotated, the left and right cam operate the sequence. The two bars move out of phase, alternatively locking and releasing the follower and memory elements, adapted from [58].

surrounding tissue. Apart from the risk of injury, poor path-following may also result in longer procedure times, thereby increasing cost [74], [75]. With this in mind, it is naturally of interest to compare FTL devices found in the literature by their relative leader-following capability. This section further compares the reported procedure times, the forces exerted by devices on their environments, and their sizes.

Different metrics may be used to evaluate the path-following ability of a device, such as a root mean square (RMS) error [65] or an overlaid motion footprint [57]. The most common metric, however, is the deviation of the device from its intended path, expressed either as an absolute value or as a percentage of the insertion length of the device being evaluated (Fig. 7). Many publications do not provide a quantitative assessment of path-following ability, and path deviation depends heavily upon many factors, such as propagation speed, insertion length, and the number and nature of the curves along the path. This makes it difficult to meaningfully identify relationships between device classifications and leader-following ability. Nevertheless, it is interesting to gain a qualitative insight into the capabilities of devices proposed in the literature. Table I shows the deviation values for nine of the devices found in the literature.

Another important aspect is the ability of the device to precisely follow the described path not only during the device insertion but also during retraction. Only a handful of papers explicitly stated that the device is capable of reversed FTL motion [24], [28], [36], [40], [43], [50], [57]–[59]. Concentric tubes [59] or alternating devices, such as the HARP [36], [43], can reverse the advancing order of the concentric elements, whereas manually-actuated systems are manually pulled backward [28], or the insertion movement is inverted; i.e., the crank is turned in the opposite direction [50], [57], [58]. However, even if not explicitly stated, electromechanically actuated devices with independent segments should be capable of backward motion by reversing the actuator motion.

2) Propagation Speed: To justify the use of an FTL device in a procedure that can also be carried out conventionally, the device should potentially be safer, more accurate, and enable faster procedure times. The decrease in time, in fact, should not compromise the procedure safety, and the device should not damage the surrounding tissues but rather increase

TABLE I
DEVIATION FROM THE PROPAGATION PATH REPORTED BY NINE FTL DEVICES FOUND IN THE LITERATURE

	Deviation (mm)			Deviation (%)		
First author (year)	Min.	Mean	Max.	Min.	Mean	Max.
Dupourqué (2019)	-	0.54	-	-	0.27	-
Chen (2014)	13.50	15.00	29.50	1.50	1.60	3.20
Zhang (2019)	2.00	3.35	4.80	1.20	1.60	2.90
Gilbert (2015)	-	2.00	-	-	2.50	-
Amanov (2019)	-	-	-	-	2.60	14.00
Amanov (2017)	6.70	5.00	10.00	9.60	7.10	14.00
Gao (2019)	0.16	-	1.78	0.27	-	3.00
Granna (2016)	-	-	0.81	-	-	5.00
Henselmans (2019)	15.00	-	40.00	13.00	-	36.00

Publications reporting path deviation data provided either the absolute value in mm (shown in columns 2-4) or as the deviation per unit inserted length, reported in percent (columns 5-7). Table sorted in ascending order of mean percentage deviation. Unreported data are marked with a "-".

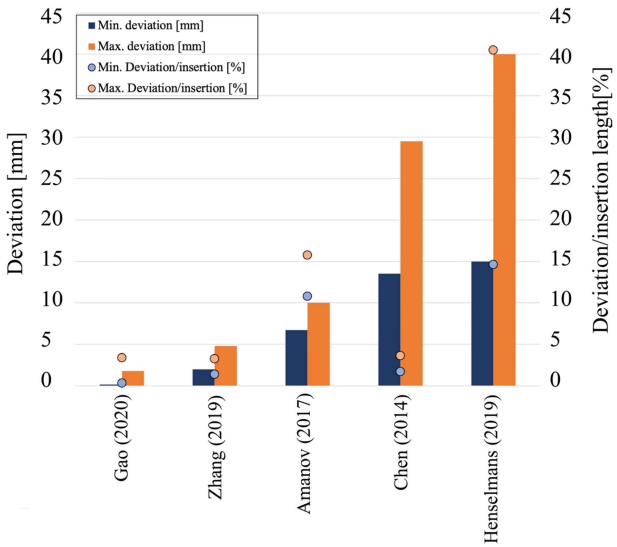

Fig. 7. Accuracy comparison of the devices that explicitly reported the deviation from the path of the device. The minimum (blue) and maximum (orange) deviation are shown as bars. The dot markers show deviation as a percentage of insertion length, where blue signifies the minimum absolute value and orange is the maximum absolute value. The two devices with the lowest reported deviation steer the leader with cables from outside the body, advance in a shifting manner with linear actuators, and apply a software constraint to the device.

the accuracy of the procedure. Propagation speed, however, is often not explicitly reported as a performance metric and can be affected by the surgeon's experience, and most of the literature deals with an early-stage technology not yet optimized for speed. Information on procedure time is mentioned in only a few publications presenting pre-clinical studies and clinical trial results. The FTL system proposed by Gao *et al.* [56], for example, shows an increased procedure time when performing a ventriculostomy and tumor biopsy in patients with normal anatomy, whereas reporting a significantly reduced procedure time in patients with abnormal anatomy. The HARP device proposed by Degani *et al.* [53], [54] reports procedure times comparable to operations performed with other robotic platforms for epiglottectomy on a cadaver [76].

3) Tissue Reaction Force and Operating Force: Another relevant performance metric is the magnitude of the forces exerted on the device's surrounding anatomical structures. By decreasing the force applied to the surrounding tissues, potential damage to these tissues can be reduced [37], [55]. Again, only a few publications measured and reported this aspect. For example, the robotic catheter for transbronchial biopsy proposed by Dupourqué *et al.* reduced the reaction forces measured with a force sensor on the phantom wall from 0.94 N with a manual catheter to 0.13 N and the average path deviation from 0.95 mm to 0.54 mm [55].

The operating forces of some devices are also measured to assess the possibility of supporting other equipment, ensuring stability during the procedure. For example, the robotic endoscope proposed by Lee *et al.* [37] allows the insertion of medical instruments through the central lumen of the device while holding a load of up to 15 N applied either axially or laterally at the distal tip of the device without changing its shape. This was manually measured using a push/pull gauge applied to the end-effector of the device. Likewise, Kang *et al.* stated that their device, shown in Fig. 6(d), ensures an operating force of approximately 4-8 N at an advancement speed of 1.5 mm/s [36]. In this case, the force was measured by externally pushing the device end-effector with a force sensor constrained to a linear stage.

4) Size: One of the major determinants of potential applications for a flexible medical device is the device's shaft diameter, and 19 publications were found that explicitly reported the diameters and lengths of their respective proposed devices. On the one hand, the shaft diameter is directly related to the surgical application the device is designed for. When the application is for instance in the gastrointestinal tract, the device can reach a diameter of 13 mm [77], whereas in applications such as neurosurgery 3.5 mm in diameter is the maximum [56]. On the other hand, the mechanism used to achieve FTL motion also requires a certain minimum shaft diameter. It was found that devices with actuators located inside the body (Fig. 8, actuator location "A") have larger diameters than devices with actuators located outside the body (Fig. 8, actuator location "B"). Pre-curved concentric tube devices with elastic relaxation as steering mechanism (Fig. 8, steering mechanism "c") have the

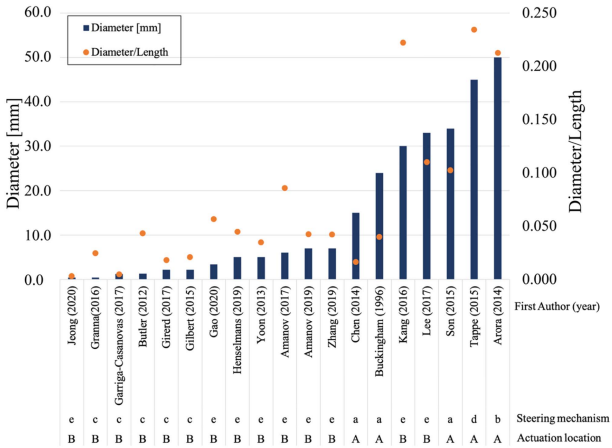

Fig. 8. Size comparison of the devices with explicitly reported maximum diameter and length, in ascending order of shaft diameter (blue bars). The orange markers show the ratio of diameter to length of each device. The first authors and the device classification are shown underneath the graph; A: actuators inside the body, B: actuators outside the body, a: motor torque force, b: thermal deformation force, c: elastic relaxation force, d: electromagnetic force, e: cable tension force.

smallest diameters, followed by devices that apply cable tension (Fig. 8, steering mechanism "e") from outside the body. Notable exceptions are the devices proposed by Kang *et al.* [36], which has no steering actuators but six shape locking actuators for each segment located inside the body, and the one proposed by Lee *et al.* [37], which is originally designed for NOTES and for which the authors propose many potential size reduction options.

5) Medical Applications: FTL devices have been developed for different medical fields due to the ability to move through tortuous paths and avoid obstacles (Fig. 9). Gastrointestinal applications such as gastroscopy or colonoscopy are one of the major application fields [26], [31], [39], [40]. Conventional flexible endoscopes are passively inserted into the colon. However, high forces can be applied to the colon walls increasing the patient's discomfort and creating difficulties for the clinician [78]. Having active navigation during colonoscope insertion would avoid high stress to the colon walls and open new possibilities in diagnostic and treatment for gastrointestinal pathologies. Chen *et al.* [23] proposed an FTL device able to follow the curves of the colon without relying on the anatomical wall and therefore simplifying the insertion, decreasing the chance of wall damage and patient discomfort. Other examples of FTL systems are the device by Gao *et al.* [56] and Yoon *et al.* [47] that find their application in neurosurgery. Gao *et al.* proposed a device for endoscopic third ventriculostomy and tumor biopsy. The device uses FTL motion to minimize tissue trauma while reaching the operation site. Yoon *et al.* designed a device for endoscopic maxillary sinus surgery able to follow the tortuous path through the nasal cavity [45]. Transluminal procedures are also a possible application of FTL devices due to their ability to move in confined spaces and provide a stable platform to operate [27], [37], [58]. Bajo *et al.* proposed an FTL device for transurethral bladder resection that allows the surgeon to operate without *a priori* knowledge with full control of the end-effector DOF [52]. Another possible application is endoscopic biopsies; for example, in organs such as the lungs, the diagnostic sensitivity of biopsies - the success rate of the procedure - is lower than 25% in the peripheral airways due to the difficulties in reaching and extracting the biopsy samples [79]. Dupourqué *et al.* proposed a device for transbronchial biopsy in which the FTL motion enhances the surgeon's maneuverability in reaching the peripheral bronchi of the lungs [55]. Applications can also be found for cardiovascular surgery [54], endovascular interventions [51], and extra-vascular procedures where the FTL device cannot rely on the vessels' wall to follow the desired path [44]. Other possible applications of FTL devices are optical biopsies [65], application of cochlear implants [67], and treating epilepsy with laser ablation of the hippocampus [66].

B. Common Steering and Shape Conservation Strategies

1) Steering: A widespread design approach in the steering of FTL devices is the combination of actuators located outside the body with tendons transmitting the forces generated by the actuators to the tip of the device. All but one of the 20 devices using tendons to steer the device utilize this strategy. Looking at the published size (Fig. 8) and performance data (Table I), it becomes clear that the goal of this strategy is to use precise motor control to steer a thinner shaft, a goal achieved with some success. Whereas systems using *elastic relaxation* tend to have smaller diameters (Fig. 8), they tend to have a mediocre path deviation per unit inserted length when compared to cable *tension* based devices. The accuracy of concentric tube robots tends to be highly dependent on the task and the design of the tubes. The tube shapes are specifically designed to achieve optimal pathing and advancement towards the target [80], [81]. Therefore, these devices are often designed for a particular medical procedure that requires a path with a specific, near-constant shape, e.g., neurological procedures [82], treatment of hydrocephalus [63], a biopsy of olfactory cells [64], or cochlear implant insertion [67]. Table I shows the published path deviation data; Gilbert *et al.* [66] and Granna *et al.* [67] are both *steering/outside body*, *elastic relaxation* devices, whereas Chen *et al.* [23] utilize tendons combined with actuation inside the body.

Furthermore, SMA and EM actuators were only found to be used as actuators inside the body [25], [29], [30]. This is most likely since these technologies can create individual actuators that are smaller than standard electric motors, leading designers to attempt to integrate them into the shaft of a device. However, this strategy does not necessarily result in smaller steerable shafts; in Fig. 8, it can be seen that these devices possess diameters of over 40 mm.

2) Shape Conservation: Software constraints were found to be used by 17 out of 35 systems. These devices were universally found to use their steering actuation to conserve their shape, most likely because this is the simplest way for an electromechanically controlled system to hold its shape: if the actuator maintains its position, the device should stay in the same configuration. This simplicity precludes other additional shape locking strategies such as friction, interlocking geometry,

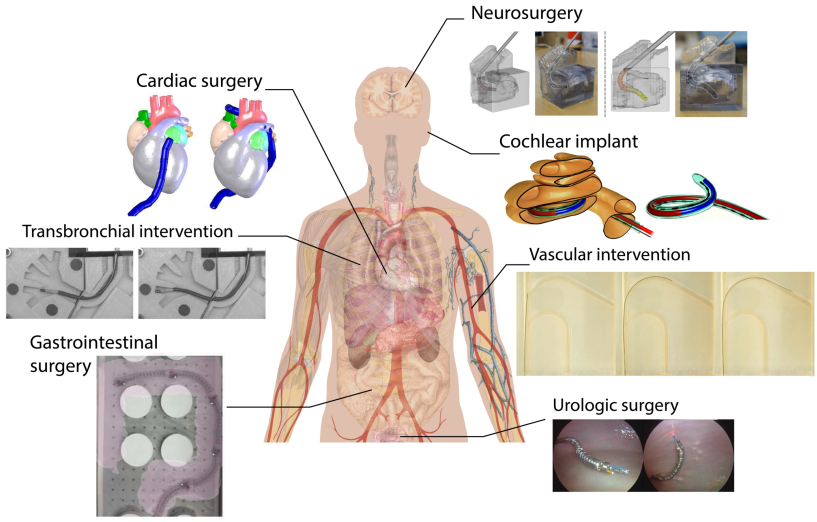

Fig. 9. Medical applications of FTL devices. Cardiac surgery, adapted from [54] (© [2006] IEEE); neurology, adapted from [45] (© [2018] IEEE); cochlear implant [67]; transbronchial intervention, adapted from [55]; vascular intervention, adapted from [51] (© [2020] IEEE); gastrointestinal surgery [23] (© [2014] IEEE); urology, adapted from [52] (© [2013] IEEE).

or elastic interactions, as they would add complexity with no real benefit.

Conversely, hardware constraints were used by 18 out of 35 devices with a variety of shape conservation strategies. For example, almost all concentric tube robots utilized their elastic relaxation properties to retain their shape, whereas geometry locking systems were engaged either by cable tension or SMA actuators. Friction locks were used exclusively by three FTL devices, such as the one shown in Fig. 4(f). All three of these devices [36], [43], [44], [53], [54] consist of alternating systems that realize FTL motion due to their ability to alternatingly advance while locking and unlocking their shape. Two mechanisms were found by which friction was translated to the stiffness of the shaft. Kang *et al.* used friction between piezoelectric clamps and tendons to prevent the tendons from moving relative to the shaft, thereby locking the system's shape [36]. On the other hand, the systems developed by Degani *et al.* and Chen *et al.* used the friction between rigid shaft elements to conserve the shape of the device [44], [53]. Degani's design applies tension on all of the steering wires simultaneously to compress the shaft elements together in the axial direction, whereas Chen's system possesses a dedicated tendon used to compress the elements together. These differing strategies further appear to affect device diameters; Chen *et al.* report a diameter of 6 mm, although as this system uses two parallel shafts, its overall diameter increases to at least 12 mm at the widest point. Degani's design is concentric, but also reports a size of 12 mm. Kang *et al.* cite a much larger diameter of 30 mm due to miniaturization limits with the piezoelectric clamps [36], supporting the argument that including any kind of actuator, even actuators that are already highly miniaturized, in the shaft of a device leads to much larger device diameters.

C. Design Combinations in FTL Devices

The designs proposed in the literature tend to cluster around certain combinations of design choices, as shown by Table II. Whereas eight combinations of the two types for each sub-function are theoretically possible (Fig. 10), only four are published. For example, every single one of the seven devices utilizing actuators inside the body controls its segments individually, enabling them to propagate in a shifting manner with software constraints. Actuation inside the body is usually less preferred than actuation outside the body due to limits in the miniaturization of the actuation components. However, with the great progress in soft robotics, new solutions can be investigated, leading to combined systems with, for example, actuation inside the body with deployment propagation.

TABLE II
EXISTING COMBINATIONS OF THE THREE FTL SUB-FUNCTIONS IN THE DEVICES FOUND IN THE LITERATURE

Sub-function 1	2	3	Description	Number of devices
A	A	A	Actuation inside body, Shifting propagation, Software constraint	7
B	A	A	Actuation outside body, Shifting propagation, Software constraint	10
B	A	B	Actuation outside body, Shifting propagation, Hardware constraint	3
B	B	B	Actuation outside body, Deploying propagation, Hardware constraint	15

Sub-functions: 1. steering, 2. propagation, 3. conservation. The devices combine types A or B from each sub-function to achieve FTL motion.

Conservation and propagation are closely related, as the manner of propagation can intrinsically provide shape conservation, particularly in systems that deploy to propagate. All of the 15 devices that advance in a deploying manner use hardware constraints to conserve the shape of the path taken by the leader/end-effector and have actuators located outside the body. Deploying devices exclusively use hardware constraints as their alternating nature means that at least one of

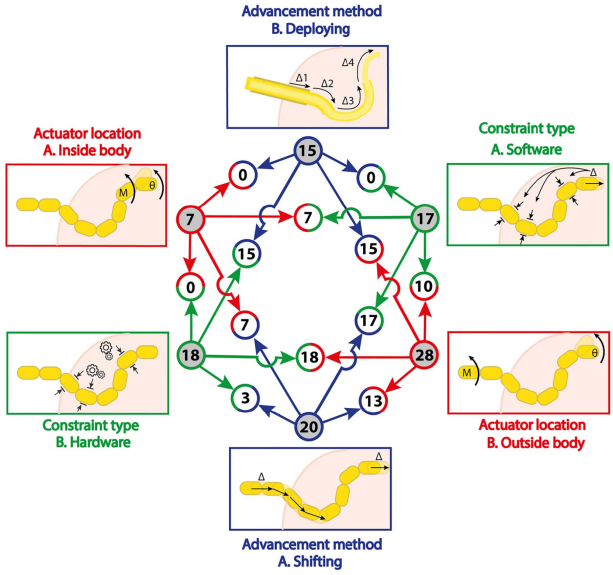

Fig. 10. Overview of combined sub-functions to achieve FTL motion in medical devices. Three FTL sub-functions steering, propagation, and conservation, associated with the colors red, blue, and green, respectively, are each executed in either type A or B. The number of devices found in the literature that are allocated to each type is noted in the grey nodes close to the schematic drawings. For example, from the 35 devices, 20 advance in a shifting manner (blue: Advancement method A. Shifting), and the remaining 15 devices advance in a deploying manner (blue: Advancement method B. Deploying). The cross combination of two sub-function types is shown in white nodes between the arrows associated with the sub-functions. The color of the perimeter and arrows correspond to the sub-function with the same color. For example, from the 20 devices that propagate in a shifting manner, seven have actuators inside the body (red arrow from A. Inside the body and blue arrow from A. Shifting), and 13 have actuators outside the body (red arrow from B. band blue arrow from A. Shifting).

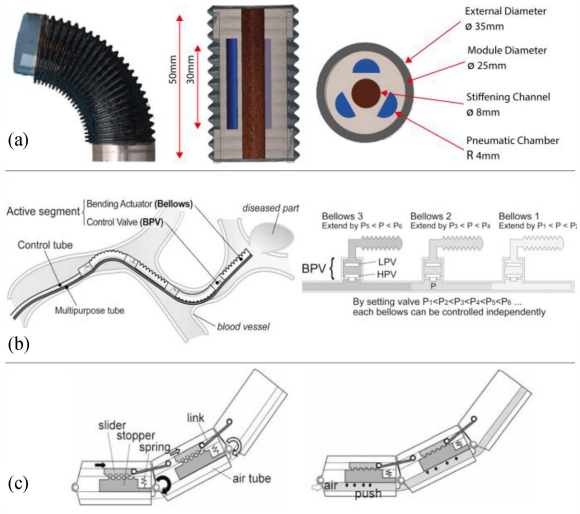

Fig. 11. Examples of medical devices with FTL potential. (a) Fluid actuated segment. Three pneumatic chambers can fill up with air. Combining the inflation of these chambers can bend the segment in various directions. If all chambers are filled, the segment elongates straightly. The stiffening channel (brown) serves as a backbone and contains coffee grains that serve as a granular interlocking substance. The grains in the stiffening channel can be compressed by a vacuum, stiffening the channel, and keeping the orientation of the segment. Adapted from [84] (© [2013] IEEE). (b) Hydraulic actuated active catheter. The catheter maneuvers through a blood vessel towards the target. The control tube supplies the fluid to all control valves. Depending on the pressure of the fluid supplied from the control tube, the valve opens, and the fluid enters the bellow, making it expand [87] (© [2012] IEEE). (c) Pneumatically actuated shape locking mechanism. When the segments bend, the links displace the sliders. The sliders contain teeth that can interlock with the stoppers. If air flows into the air tube, the air tube expands and pushes the stoppers upwards compressing the springs. The interlocking teeth prevent the sliders from moving, fixing the position of the links and therefore the orientation of the segments. If the air leaves the air tube, the compressed springs reset the stoppers downwards. Adapted from [88].

the concentric shafts always serves as a physical constraint, making software constraints redundant. Conversely, 17 of the 20 devices propagating in a shifting manner apply a software constraint, as shifting propagation requires individual control of the segments that is commonly combined with feedback control to impose software constraints as discussed in Section III-D. The remaining three devices [50], [57], [58] apply a hardware constraint to the segment shape. Unlike hardware constraints in deploying devices, hardware constraints in shifting devices are located outside the body alongside the actuation system. These constraints act directly on the actuation of a given segment. This constrained actuation is further mechanically coupled to the device translation, resulting in a shifting propagation. The devices proposed by Henselmans *et al.* have a physical track (a programmed cam or a pre-curved rod) that serves as the physical constraint for the segment actuation in the controller [50], [57]. The physically constrained actuation is then transferred with cables to the instrument shaft. Thus, relocating the concentric physical constraint mechanism to a module outside the main body results in a shifting propagation with a hardware constraint. While it is difficult to directly compare devices based on the number of DOF, the inherent expense of including additional actuators in any given robotic system makes it desirable to increase the number of DOF controllable per actuator. Most of the surveyed devices showed a ratio of between 0.5 and 1.5 DOF per actuator. Some devices with hardware constraints showed, however, a higher number of DOF per actuator. Devices with hardware constraints showed a higher number of DOF per actuator. Notable outliers are [50], [57] (with a geometry lock in the handle control), and the alternating device proposed by Degani *et al.* [53], which showed 28, 36, and 17 DOF/actuator, respectively.

D. Assessment of Alternative Solutions for FTL Medical Devices

Medical devices with FTL potential: Many devices found in the literature contain two of the three sub-functions to achieve FTL motion. Various devices with pneumatic or hydraulic actuation show potential for FTL capabilities with pneumatic or hydraulic actuators. A device excluded uses two pneumatically extensible and bendable segments in series, Fig. 11(a) [83], [84]. Steering each segment is achieved by filling the fluid chambers inside the segment, whereas their configuration is hold using granular jamming, a mechanism used in medical devices or soft robotics to adjust the system stiffness [85], [86]. Keeping

a similar configuration to the one proposed by Ranzani *et al.*, an FTL motion could have been achieved using a deploying mechanism to propagate the shape, as for the concentric tubes.

Another excluded device uses hydraulic bellows inside a catheter of 3 mm in diameter to steer the segments [87], Fig. 11(b). Depending on the pressure, the bellows stretch or shrink the segments on one side, making them bend. The system contains special valves that allow for independent control of each segment. The authors claim that the device operates with safe pressures for blood vessels and uses saline solution as a hydraulic fluid. If steering with bellows would be coupled to the displacement of the catheter, FTL motion could be achieved by steering with hydraulic forces that could also be used to hold the path configuration.

An interesting locking mechanism that could be applied for FTL motion is the pneumatic expansion of tubes to lock segments in their orientation of the device shown in Fig. 11(c) [88]. Alternating devices, such as the devices shown in Fig. 4(f) and 7(d), could use this locking mechanism to memorize the shape.

FTL motion as a combination between tool and shaft propagation: Many of the reviewed solutions are designed to act as a guide for other instruments, such as biopsy forceps. While this review focused solely on devices with the shaft that performs FTL motion, it is possible that a surgical instrument, inserted through a working channel of the shaft, could take the role of the leader segment, thereby creating a combination instrument/shaft FTL device. This could be advantageous from a human-machine interface perspective, as the forward propagation of the shaft as a whole would be intrinsically tied to the pose of the inserted instrument instead of being a separately-controlled function.

FTL devices with nonmedical applications: As stated in the introduction, many FTL devices have a nonmedical application. This often means that their design is not applicable to medical devices. A few exceptions have been found for FTL devices that have similar design constraints or have the potential to be miniaturized. The device presented by Dong *et al.* features an inspection/repair robot for gas turbines [89]. Some of the specifications are a minimum of 25 DOF, maximum tip diameter of 15 mm, and 1200 mm arm length. The device is steered with cables by actuators outside the segments, advances in a shifting manner with a motor, and applies a software constraint where the steering actuation holds the configuration. Another device, designed for search and rescue operations, uses so-called growth navigation [90], Fig. 12. The steering is achieved by increasing the length of the device on one side. A pump with air pressure supplied actuates the increase in length. The device advances in a deploying manner with air pressure, and the shape is conserved by a physical constraint where air pressure holds the configuration of the device. The device is also able to retract from a straight position.

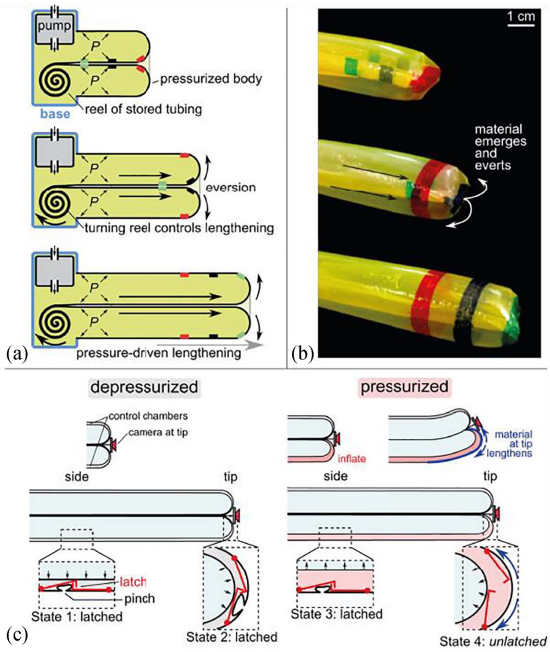

Fig. 12. Soft robot with growth navigation. (a) A schematic side-section view of the deploying robot. Air is pumped into the device, reeling out the stored tubing as it everts from the center. (b) Picture of the device. (c) Steering mechanism. The device has control chambers on the outer edge that contain a series of latches. These latches pinch the outer edge of the control chamber, essentially decreasing its length. The latches behave differently depending on their position (side or tip) and the state of the control chamber (depressurized or pressurized), giving four States. Adapted from [90].

E. Commercially Available Instruments

Four of the devices found in the literature are or were commercially available. In 1996, Buckingham and Graham presented the first prototype of a device that had servo motors embedded inside the segments [31]. According to the authors' evaluation, the manipulator had to be five times smaller and place the actuation outside the main body of the device to be used for surgeries. The authors suggested having a device with actuators outside the shaft would help miniaturization. In 2002 Buckingham presented the commercialized version of the prototype proposed in 1996: OC Robotics. The OC Robotics 10 DOF snake arm robot is a tendon-driven device with actuators outside the shaft and is commercially available for search and rescue or repair operations [91]. In 2003, OC Robotics patented FTL technology for medical devices [38] and was awarded for NOTES robotic development in 2011 [92]. OC Robotics was mentioned in a review in 2012 [93], including one medical device, but so far, there are no FTL medical devices commercially available from OC Robotics.

Another patented device presented by Saadat *et al.* is affiliated with USGI Medical [39]. The patent contains a shape locking mechanism that is used in the commercially available catheter from USGI medical [94]. However, the commercialized catheter does not have a propagating mechanism and associated shape conservation method as described in the patent.

Another device was patented by Donhowe *et al.* [40] in 2013 and today is commercially provided by Intuitive Surgical as Ion^{TM} [95]. The device, used in bronchoscopy to perform biopsies in the lungs, has a shaft diameter of 3.5 mm and uses path planning before the intervention with the help of a computed tomography scan to pre-plan its insertion and the retraction.

The path is, therefore, predefined and cannot be changed during navigation. Moreover, Ion^{TM} bases its propagation on the surrounding anatomies, and a shape lock mechanism provides rigid support for the biopsy needle. A fiber optic shape sensor measures the full shape of the device during the insertion. A multicenter study is ongoing, but positive preliminary results have already been published [96], [97].

Virtuoso surgical is a start-up [98] basing its technology on the concentric tube robot presented in the work of Gilbert *et al.* [66]. The system is intended to enhance dexterity compared to rigid endoscopes when operating in a single port surgery. Even if the FTL motion seems to have not yet been implemented in the system, future works could propose new generations of endoscopes able to follow and memorize the desired path.

Finally, the HARP, presented by Degani *et al.* (Fig. 4(f)), is provided by Medrobotics (MA, USA) as Flex Robotic System [99]. The Flex Robotic System has been tested in cadaveric transoral surgery [76] and evaluated in its performance in various studies [100], showing promising results in colon rectus inspections and in transoral procedures where the mouth is used as the entry port for the surgical procedure [101], [102].

F. The Future of FTL Medical Devices

Most of the works analyzed in this review, 35 out of 43, have been published within the last ten years. This indicates that the field of FTL medical devices is still in the development phase and that new solutions are expected in the upcoming years. With the advent of soft robotics, research on new materials is being carried out, opening the way to new possibilities for FTL devices. Shape memory alloys (SMA) are widely used in the medical field due to their MRI- and bio-compatibility. In this review, an example of their application is given by Arora *et al.* [25] that use SMA wires to steer their device. Electro-active polymers (EAP) change their stiffness depending on the applied voltage, and they represent a valid alternative to conventional actuation methods. However, even if widely used in general purpose soft robotics [103], EAP scarcely find their application in medical devices due to their need for high voltage, low response time, and low exerted forces [104]. Elastomers such as polydimethylsiloxane (PDMS) are often used in soft robotic systems for minimally invasive surgery [104] due to their low cost, easy availability, and MRI-compatibility. Elastomers are often used in Flexible Fluidic Actuators (FFA), allowing changes in stiffness using air or liquids and avoiding electrical sources [105], [106]. These properties could be used to create an FTL motion in concentric mechanisms. Interesting materials that find application in medical devices are hydrogels. Hydrogels respond to temperature, chemical, magnetic, or electrical stimuli by expanding or shrinking, changing their rigidity and shape [107]. Interesting results have been achieved in the fabrication of soft grippers [108], [109], showing potential for FTL medical devices.

An important aspect that must be taken into consideration is the use of devices as disposable or reusable instruments. Looking at robotic systems, such as the da Vinci robotic system (Intuitive Surgical Inc., Sunnyvale, CA, USA), having robotic arms with embedded electronics and miniaturized components leads to a short life span for the instruments and high costs of maintenance [110]. In this scenario, additive manufacturing technology, also known as 3D printing, could open new opportunities for disposable and customized shafts and end-effectors due to the possibility of modifying the design considering surgeon's and patient's needs [111]–[113]. The implementation of this new technology, together with the implementation of FTL motion in surgical devices, represents a step forward to more personalized medicine.

V. Conclusion

FTL motion was divided into three fundamental sub-functions: steering, propagation, and conservation. As each sub-function has two types of solutions, eight combinations are possible, of which only half were found in the literature. Despite being often proposed in medical devices, no FTL devices were found based on pneumatic mechanisms. Device specifications were mostly task-specific although some patterns were apparent for certain design choices. For example, a smaller diameter was chosen for devices with actuators outside the body, in particular pre-curved concentric tube devices. The largest number of DOF per actuator was achieved by devices using hardware constraints to conserve their shape. FTL devices have great potential in the medical field, especially in procedures with abnormal anatomies and unpredictable situations. In this work, we provided a detailed overview of the solutions currently available for FTL devices, reflecting on current limitations and future perspectives. This review offers the foundation that will aid in the development of an innovative generation of medical devices.

References

[1] P. Gavriilidis and K. Katsanos, "Laparoscopic versus open transverse colectomy: A systematic review and meta-analysis," *World J. Surg.*, vol. 42, no. 9, pp. 3008–3014, 2018, doi: 10.1007/s00268-018-4570-5.

[2] J. A. Warren and M. Love, "Incisional hernia repair: Minimally invasive approaches," *Surg. Clin. North Amer.*, vol. 98, no. 3, pp. 537–559, 2018, [Online]. Available: https://doi.org/10.1016/j.suc.2018.01.008.

[3] M. Honda *et al.*, "Surgical risk and benefits of laparoscopic surgery for elderly patients with gastric cancer: A multicenter prospective cohort study," *Gastric Cancer*, vol. 22, no. 4, pp. 845–852, 2019, doi: 10.1007/s10120-018-0898-7.

[4] N. Kulkarni and T. Arulampalam, "Laparoscopic surgery reduces the incidence of surgical site infections compared to the open approach for colorectal procedures: A meta-analysis," *Tech. Coloproctol.*, vol. 24, no. 10, pp. 1017–1024, 2020, doi: 10.1007/s10151-020-02293-8.

[5] T. Xu, S. M. Hutfless, M. A. Cooper, M. Zhou, A. B. Massie, and M. A. Makary, "Hospital cost implications of increased use of minimally invasive surgery," *JAMA Surg.*, vol. 150, no. 5, pp. 489–490, 2015.

[6] H. Hwang, J.-E. Myung, J. W. Yi, S.-S. Lee, and J. Park, "Laparoscopic surgery versus open surgery for gastric cancer: Big data analysis based on nationwide administrative claims data," *Ann. Surg. Treat. Res.*, vol. 99, no. 3, pp. 138–145, Sep. 2020, doi: 10.4174/astr.2020.99.3.138.

[7] Z. Mitros, B. Thamo, C. Bergeles, L. da Cruz, K. Dhaliwal, and M. Khadem, "Design and modelling of a continuum robot for distal lung sampling in mechanically ventilated patients in critical care," *Front. Robot. AI*, vol. 8, May 2021, Art. no. 611866, doi: 10.3389/frobt.2021.611866.

[8] B. M. Shrestha, "Natural orifice transluminal endoscopic surgery (NOTES)-an emerging technique in surgery," *J. Nepal Med. Assoc.*, vol. 51, no. 184, pp. 456–459, 2011.

[9] B. Azizi Koutenaei, E. Wilson, R. Monfaredi, C. Peters, G. Kronreif, and K. Cleary, "Robotic natural orifice transluminal endoscopic surgery (R-NOTES): Literature review and prototype system," *Minim. Invasive Ther. Allied Technol.*, vol. 24, no. 1, pp. 18–23, 2015.

[10] B. Dallemagne, S. Perretta, P. Allemann, M. Asakuma, and J. Marescaux, "Transgastric hybrid cholecystectomy," *Brit. J. Surg. Inc. Eur. J. Surg. Swiss Surg.*, vol. 96, no. 10, pp. 1162–1166, 2009.
[11] T. Rahimli, T. Hidayetov, Z. Yusifli, H. Memmedzade, T. Rajabov, and K. Aghayev, "Endoscopic endonasal approach to giant pituitary adenomas. Surgical outcomes and review of the literature.," *World Neurosurg.*, vol. 149, pp. e1043–e1055, 2021.
[12] L. Blanc, A. Delchambre, and P. Lambert, "Flexible medical devices: Review of controllable stiffness solutions," *Actuators*, vol. 6, no. 3, pp. 1–31, 2017.
[13] A. Loeve, P. Breedveld, and J. Dankelman, "Scopes too flexible … and too stiff," *IEEE Pulse*, vol. 1, no. 3, pp. 26–41, Nov./Dec. 2010.
[14] H. Choset and W. Henning, "A follow-the-leader approach to serpentine robot motion planning," *ASCE J. Aerosp. Eng.*, vol. 12, no. 2, pp. 65–73, 1999.
[15] J. Burgner-Kahrs, D. C. Rucker, and H. Choset, "Continuum robots for medical applications: A survey," *IEEE Trans. Robot.*, vol. 31, no. 6, pp. 1261–1280, Dec. 2015, doi: 10.1109/TRO.2015.2489500.
[16] H. Komura, H. Yamada, and S. Hirose, "Development of snake-like robot ACM-R8 with large and mono-tread wheel," *Adv. Robot.*, vol. 29, no. 17, pp. 1081–1094, 2015.
[17] P. Liljebäck, K. Y. Pettersen, Ø. Stavdahl, and J. T. Gravdahl, "A review on modelling, implementation, and control of snake robots," *Rob. Auton. Syst.*, vol. 60, no. 1, pp. 29–40, 2012.
[18] Z. Cao, D. Zhang, B. Hu, and J. Liu, "Adaptive path following and locomotion optimization of snake-like robot controlled by the central pattern generator," *Complexity*, vol. 2019, no. 2, pp. 1–13, 2019.
[19] G. Granosik and J. Borenstein, "Integrated joint actuator for serpentine robots," *IEEE/ASME Trans. Mechatron.*, vol. 10, no. 5, pp. 473–481, Oct. 2005.
[20] S. Inagaki, T. Niwa, and T. Suzuki, "Follow-the-contact-point gait control of centipede-like multi-legged robot to navigate and walk on uneven terrain," in *Proc. IEEE/RSJ Int. Conf. Intell. Robots Syst.*, 2010, pp. 5341–5346.
[21] L. Tang, J. Wang, Y. Zheng, G. Gu, L. Zhu, and X. Zhu, "Design of a cable-driven hyper-redundant robot with experimental validation," *Int. J. Adv. Robot. Syst.*, vol. 14, no. 5, 2017, Art. no. 1729881417734458.
[22] Q. Fu and C. Li, "Robotic modelling of snake traversing large, smooth obstacles reveals stability benefits of body compliance," *R. Soc. Open Sci.*, vol. 7, no. 2, 2020, Art. no. 191192.
[23] Y. Chen, J. Liang, and I. W. Hunter, "Modular continuum robotic endoscope design and path planning," in *Proc. IEEE Int. Conf. Robot. Automat.*, 2014, pp. 5393–5400.
[24] D. Palmer, S. Cobos-Guzman, and D. Axinte, "Real-time method for tip following navigation of continuum snake arm robots," *Rob. Auton. Syst.*, vol. 62, no. 10, pp. 1478–1485, 2014.
[25] A. Arora, Y. Ambe, T. H. Kim, R. Ariizumi, and F. Matsuno, "Development of a maneuverable flexible manipulator for minimally invasive surgery with varied stiffness," *Artif. Life Robot.*, vol. 19, no. 4, pp. 340–346, 2014.
[26] K. Ikuta, M. Tsukamoto, and S. Hirose, "Shape memory alloy servo actuator system with electric resistance feedback and application for active endoscope," in *Proc. IEEE Int. Conf. Robot. Autom.*, 1988, pp. 427–430.
[27] K.-W. Kwok *et al.*, "Dimensionality reduction in controlling articulated snake robot for endoscopy under dynamic active constraints," *IEEE Trans. Robot.*, vol. 29, no. 1, pp. 15–31, Feb. 2013, doi: 10.1109/TRO.2012.2226382.
[28] J. Son *et al.*, "A novel semi-automatic snake robot for natural orifice transluminal endoscopic surgery: Preclinical tests in animal and human cadaver models (with video)," *Surg. Endosc.*, vol. 29, no. 6, pp. 1643–1647, 2015.
[29] S. Tappe, J. Pohlmann, J. Kotlarski, and T. Ortmaier, "Towards a follow-the-leader control for a binary actuated hyper-redundant manipulator," in *Proc. IEEE Int. Conf. Intell. Robots Syst.*, 2015, pp. 3195–3201, doi: 10.1109/IROS.2015.7353820.
[30] S. Tappe, J. Kotlarski, T. Ortmaier, M. Dörbaum, A. Mertens, and B. Ponick, "The kinematic synthesis of a spatial, hyper-redundant system based on binary electromagnetic actuators," in *Proc. 6th Int. Conf. Automat., Robot. Appl.*, 2015, pp. 211–216.
[31] R. O. Buckingham and A. C. Graham, "Computer controlled redundant endoscopy," in *Proc. IEEE Int. Conf. Syst., Man Cybern.. Inf. Intell. Syst.*, 1996, pp. 1779–1783.
[32] J. M. Jani, M. Leary, A. Subic, and M. A. Gibson, "A review of shape memory alloy research, applications and opportunities," *Mater. Des.*, vol. 56, pp. 1078–1113, 2014.
[33] M. M. Kheirikhah, S. Rabiee, and M. E. Edalat, "A review of shape memory alloy actuators in robotics," in *Proc. Robot Soccer World Cup*, 2010, pp. 206–217.
[34] M. A. Qidwai and D. C. Lagoudas, "On thermomechanics and transformation surfaces of polycrystalline niti shape memory alloy material," *Int. J. Plast.*, vol. 16, no. 10/11, pp. 1309–1343, 2000.
[35] E. Amanov, J. Granna, and J. Burgner-Kahrs, "Toward improving path following motion: Hybrid continuum robot design," in *Proc. IEEE Int. Conf. Robot. Automat.*, 2017, pp. 4666–4672.
[36] B. Kang, R. Kojcev, and E. Sinibaldi, "The first interlaced continuum robot, devised to intrinsically follow the leader," *PLoS One*, vol. 11, no. 2, 2016, Art. no. e0150278.
[37] H. Lee, K. G. Kim, J. H. Seo, and D. K. Sohn, "Natural orifice transluminal endoscopic surgery with a snake-mechanism using a movable pulley," *Int. J. Med. Robot. Comput. Assist. Surg.*, vol. 13, no. 4, 2017, Art. no. e1816.
[38] R. Buckingham and A. Graham, "Robotic positioning of a work tool or sensor," United State Patent 10/370,190, Dec. 11, 2003.
[39] V. Saadat, R. C. Ewers, and E. G. Chen, "Shape lockable apparatus and method for advancing an instrument through unsupported anatomy," in *Google Patents*, San Francisco, CA, USA: USGI Medical, Inc., Sep. 2004.
[40] C. Q. Donhowe *et al.*, "Method and system for steerable medical device path definition and following during insertion and retraction." US Patent 9913572, Oct. 2013.
[41] M. Neumann and J. Burgner-Kahrs, "Considerations for follow-the-leader motion of extensible tendon-driven continuum robots," in *Proc. IEEE Int. Conf. Robot. Automat.*, 2016, pp. 917–923, doi: 10.1109/ICRA.2016.7487223.
[42] T. D. Nguyen and J. Burgner-Kahrs, "A tendon-driven continuum robot with extensible sections," in *Proc. IEEE Int. Conf. Intell. Robots Syst.*, 2015, pp. 2130–2135, doi: 10.1109/IROS.2015.7353661.
[43] H. M. Choset, A. Wolf, and M. A. Zenati, "Steerable, follow the leader device," in *Google Patents*, San Francisco, CA, USA: USGI Medical, Inc., Dec. 2018.
[44] Y. Chen, J. H. Chang, A. S. Greenlee, K. C. Cheung, A. H. Slocum, and R. Gupta, "Multi-turn, tension-stiffening catheter navigation system," in *Proc. IEEE Int. Conf. Robot. Automat.*, 2010, pp. 5570–5575.
[45] H.-S. Yoon, J. H. Jeong, and B.-J. Yi, "Image-Guided dual master–slave robotic system for maxillary sinus surgery," *IEEE Trans. Robot.*, vol. 34, no. 4, pp. 1098–1111, Aug. 2018, doi: 10.1109/TRO.2018.2830334.
[46] E. Amanov, T.-D. Nguyen, and J. Burgner-Kahrs, "Tendon-driven continuum robots with extensible sections—A model-based evaluation of path-following motions," *Int. J. Rob. Res.*, vol. 40, no. 1, 2019, Art. no. 0278364919886047.
[47] H.-S. Yoon, H.-J. Cha, J. Chung, and B.-J. Yi, "Compact design of a dual master-slave system for maxillary sinus surgery," in *Proc. IEEE/RSJ Int. Conf. Intell. Robots Syst.*, 2013, pp. 5027–5032.
[48] H.-S. Yoon and B.-J. Yi, "A 4-DOF flexible continuum robot using a spring backbone," in *Proc. Int. Conf. Mechatronics Automat.*, 2009, pp. 1249–1254.
[49] Z. Zhang, J. Dequidt, J. Back, H. Liu, and C. Duriez, "Motion control of cable-driven continuum catheter robot through contacts," *IEEE Robot. Autom. Lett.*, vol. 4, no. 2, pp. 1852–1859, Apr. 2019.
[50] P. W. J. Henselmans, C. Culmone, D. J. Jager, R. I. B. van Starkenburg, and P. Breedveld, "The memoflex II, a non-robotic approach to follow-the-leader motion of a snake-like instrument for surgery using four predetermined physical tracks," *Med. Eng. Phys.*, vol. 86, pp. 86–95, 2020. [Online]. Available: https://doi.org/10.1016/j.medengphy.2020.10.013
[51] S. Jeong, Y. Chitalia, and J. P. Desai, "Design, modeling, and control of a coaxially aligned steerable (COAST) guidewire robot," *IEEE Robot. Autom. Lett.*, vol. 5, no. 3, pp. 4947–4954, Jul. 2020.
[52] A. Bajo, R. B. Pickens, S. D. Herrell, and N. Simaan, "Constrained motion control of multisegment continuum robots for transurethral bladder resection and surveillance," in *Proc. IEEE Int. Conf. Robot. Automat.*, 2013, pp. 5837–5842.
[53] A. Degani, H. Choset, A. Wolf, and M. A. Zenati, "Highly articulated robotic probe for minimally invasive surgery," in *Proc. 2006 IEEE Int. Conf. Robot. Automat.,* 2006, pp. 4167–4172.
[54] A. Degani, H. Choset, A. Wolf, T. Ota, and M. A. Zenati, "Percutaneous intrapericardial interventions using a highly articulated robotic probe," in *Proc. IEEE/RAS-EMBS Int. Conf. Biomed. Robot. Biomechatronics*, 2006, pp. 7–12.

[55] L. Dupourqué, F. Masaki, Y. L. Colson, T. Kato, and N. Hata, "Transbronchial biopsy catheter enhanced by a multisection continuum robot with follow-the-leader motion," *Int. J. Comput. Assist. Radiol. Surg.*, vol. 14, no. 11, pp. 1–9, 2019.

[56] Y. Gao, K. Takagi, T. Kato, N. Shono, and N. Hata, "Continuum robot with follow the leader motion for endoscopic third ventriculostomy and tumor biopsy," *IEEE Trans. Biomed. Eng.*, vol. 67, no. 2, pp. 379–390, Feb. 2020.

[57] P. W. J. Henselmans, G. Smit, and P. Breedveld, "Mechanical Follow-the-Leader motion of a hyper-redundant surgical instrument: Proof-of-concept prototype and first tests," *Proc. Inst. Mech. Eng. Part H J. Eng. Med.*, vol. 233, no. 11, 2019, Art. no. 0954411919876466.

[58] P. W. J. Henselmans, S. Gottenbos, G. Smit, and P. Breedveld, "The memo slide : An explorative study into a novel mechanical follow-the- leader mechanism," *Proc. Inst. Mech. Eng. Part H J. Eng. Med.*, vol. 231, no. 12, pp. 1213–1223, 2017, doi: 10.1177/0954411917740388.

[59] B. Qi, Z. Yu, Z. K. Varnamkhasti, Y. Zhou, and J. Sheng, "Toward a telescopic steerable robotic needle for minimally invasive tissue biopsy," *IEEE Robot. Autom. Lett.*, vol. 6, no. 2, pp. 1989–1996, Apr. 2021.

[60] I. D. Walker, "Continuous backbone 'Continuum' robot manipulators," *ISRN Robot,* vol. 2013, no. 1, pp. 1–19, 2013, doi: 10.5402/2013/726506.

[61] F. Campisano *et al.*, "Closed-loop control of soft continuum manipulators under tip follower actuation," *Int. J. Rob. Res.*, vol. 40, no. 6/7, pp. 923–938, Mar. 2021, doi: 10.1177/0278364921997167.

[62] C. Bergeles, A. H. Gosline, N. V. Vasilyev, P. J. Codd, J. Pedro, and P. E. Dupont, "Concentric tube robot design and optimization based on task and anatomical constraints," *IEEE Trans. Robot.*, vol. 31, no. 1, pp. 67–84, Feb. 2015.

[63] E. J. Butler *et al.*, "Robotic neuro-emdoscope with concentric tube augmentation," in *Proc. IEEE/RSJ Int. Conf. Intell. Robots Syst.*, 2012, pp. 2941–2946.

[64] C. Girerd, A. V. Kudryavtsev, P. Rougeot, P. Renaud, K. Rabenorosoa, and B. Tamadazte, "SLAM-Based Follow-the-Leader deployment of concentric tube robots," *IEEE Robot. Autom. Lett.*, vol. 5, no. 2, pp. 548–555, Apr. 2020.

[65] C. Girerd, K. Rabenorosoa, P. Rougeot, and P. Renaud, "Towards optical biopsy of olfactory cells using concentric tube robots with follow-the-leader deployment," in *Proc. IEEE/RSJ Int. Conf. Intell. Robots Syst.*, 2017, pp. 5661–5887.

[66] H. B. Gilbert, J. Neimat, and R. J. Webster, "Concentric tube robots as steerable needles: Achieving follow-the-leader deployment," *IEEE Trans. Robot.*, vol. 31, no. 2, pp. 246–258, Apr. 2015, doi: 10.1109/TRO.2015.2394331.

[67] J. Granna, T. S. Rau, T.-D. Nguyen, T. Lenarz, O. Majdani, and J. Burgner-Kahrs, "Toward automated cochlear implant insertion using tubular manipulators," in *Proc. Med. Imag. 2016: Image-Guided Procedures, Robotic Interv., Model.*, 2016, Art. no. 97861F.

[68] P. Sears and P. Dupont, "A steerable needle technology using curved concentric tubes," in *Proc. IEEE/RSJ Int. Conf. Intell. Robots Syst.*, 2006, pp. 2850–2856.

[69] A. Garriga-Casanovas and F. Rodriguez y Baena, "Complete follow-the-leader kinematics using concentric tube robots," *Int. J. Rob. Res.*, vol. 37, no. 1, pp. 197–222, 2018.

[70] J. Burgner-Kahrs, H. B. Gilbert, J. Granna, P. J. Swaney, and R. J. Webster, "Workspace characterization for concentric tube continuum robots," in *Proc. IEEE/RSJ Int. Conf. Intell. Robots Syst.*, 2014, pp. 1269–1275.

[71] A. W. Mahoney, H. B. Gilbert, and R. J. Webster III, "A review of concentric tube robots: Modeling, control, design, planning, and sensing (volume 1: Minimally invasive surgical robotics)," in *Encyclopedia of Medical Robotics*. China: Global Publishing, 2019, pp. 181–202.

[72] H. B. Gilbert, D. C. Rucker, and R. J. Webster, III, "Concentric tube robots: The state of the art and future directions," in *Robotics Research*, New York, NA, USA: Springer, 2016, pp. 253–269.

[73] H. B. Gilbert and R. J. Webster, "Can concentric tube robots follow the leader?," in *Proc. IEEE Int. Conf. Robot. Automat.*, 2013, pp. 4881–4887, doi: 10.1109/ICRA.2013.6631274.

[74] R. E. Perez and S. D. Schwaitzberg, "Robotic surgery: Finding value in 2019 and beyond," *Ann. Laparosc. Endosc. Surg.*, vol. 4, pp. 1–7, 2019.

[75] I. G. Jeong *et al.*, "Association of robotic-assisted vs laparoscopic radical nephrectomy with perioperative outcomes and health care costs, 2003 to 2015," *Jama*, vol. 318, no. 16, pp. 1561–1568, 2017.

[76] P. J. Johnson *et al.*, "Demonstration of transoral surgery in cadaveric specimens with the medrobotics flex system," *Laryngoscope*, vol. 123, no. 5, pp. 1168–1172, 2013.

[77] M. Kay and R. Wyllie, *Colonoscopy, Polypectomy, and Related Techniques*, R. Wyllie and J. S. B. T.-P. G. and L. D. F. E. Hyams, Eds. Saint Louis, MO, USA: W.B. Saunders, 2011, pp. 650–667.e2.

[78] A. J. Loeve, P. Fockens, and P. Breedveld, "Mechanical analysis of insertion problems and pain during colonoscopy: Why highly skill-dependent colonoscopy routines are necessary in the first place … and how they may be avoided," *Can. J. Gastroenterol.*, vol. 27, no. 5, pp. 293–302, 2013.

[79] D. P. Steinfort, Y. H. Khor, R. L. Manser, and L. B. Irving, "Radial probe endobronchial ultrasound for the diagnosis of peripheral lung cancer: Systematic review and meta-analysis," *Eur. Respir. J.*, vol. 37, no. 4, pp. 902–910, 2011.

[80] C. Bedell, J. Lock, A. Gosline, and P. E. Dupont, "Design optimization of concentric tube robots based on task and anatomical constraints," in *Proc. IEEE Int. Conf. Robot. Automat.*, 2011, pp. 398–403.

[81] J. Burgner *et al.*, "A telerobotic system for transnasal surgery," *IEEE/ASME Trans. Mechatron.*, vol. 19, no. 3, pp. 996–1006, Jun. 2014.

[82] X. Yang, S. Song, L. Liu, T. Yan, and M. Q.-H. Meng, "Design and optimization of concentric tube robots based on surgical tasks, anatomical constraints and Follow-the-Leader deployment," *IEEE Access*, vol. 7, pp. 173612–173625, 2019.

[83] T. Ranzani, G. Gerboni, M. Cianchetti, and A. Menciassi, "A bioinspired soft manipulator for minimally invasive surgery," *Bioinspiration Biomimetics*, vol. 10, no. 3, 2015, Art. no. 035008, doi: 10.1088/1748-3190/10/3/035008.

[84] M. Cianchetti, T. Ranzani, G. Gerboni, I. De Falco, C. Laschi, and A. Menciassi, "STIFF-FLOP surgical manipulator: Mechanical design and experimental characterization of the single module," in *Proc. IEEE/RSJ Int. Conf. Intell. robots Syst.*, 2013, pp. 3576–3581.

[85] L. Blanc, A. Pol, B. François, A. Delchambre, P. Lambert, and F. Gabrieli, "Granular jamming as controllable stiffness mechanism for medical devices," in *Micro to MACRO Mathematical Modelling in Soil Mechanics*, New York, NA, USA: Springer, 2018, pp. 57–66.

[86] N. G. Cheng *et al.*, "Design and analysis of a robust, low-cost, highly articulated manipulator enabled by jamming of granular media," in *Proc. IEEE Int. Conf. Robot. Automat.*, 2012, pp. 4328–4333.

[87] K. Ikuta, Y. Matsuda, D. Yajima, and Y. Ota, "Pressure pulse drive: A control method for the precise bending of hydraulic active catheters," *IEEE/ASME Trans. Mechatron.*, vol. 17, no. 5, pp. 876–883, Oct. 2012.

[88] A. Yagi, K. Matsumiya, K. Masamune, H. Liao, and T. Dohi, "Rigid-flexible outer sheath model using shape lock mechanism by air pressure and wire driven curving mechanism," in *Proc. BT - World Congr. Med. Phys. Biomed. Eng. 2006*, 2007, pp. 3108–3111.

[89] X. Dong *et al.*, "Development of a slender continuum robotic system for on-wing inspection/repair of gas turbine engines," *Robot. Comput. Integr. Manuf.*, vol. 44, pp. 218–229, 2017.

[90] E. W. Hawkes, L. H. Blumenschein, J. D. Greer, and A. M. Okamura, "A soft robot that navigates its environment through growth," *Sci. Robot.*, vol. 2, no. 8, 2017, Art. no. eaan3028.

[91] R. Buckingham, "Snake arm robots," *Ind. Robot Int. J.*, vol. 29, no. 3, pp. 242–245, 2002.

[92] O. C. Robotics, "SWRDA awards OC robotics research grant to develop surgical snake-arm robot," 2011, Accessed: Feb. 22, 2021. [Online]. Available: https://www.ocrobotics.com/news/swrda-awards-oc-robotics-research-grant-to-develop-surgical-snakearm-robot

[93] R. Bloss, "Snake-like robots 'reach' into many types of applications," *Ind. Robot Int. J.*, vol. 39, no. 5, pp. 436–440, 2012.

[94] L. L. Swanstrom *et al.*, "Development of a new access device for transgastric surgery," *J. Gastrointest. Surg.*, vol. 9, no. 8, pp. 1129–1137, 2005.

[95] Intuitive Surgical, "Ion™ by Intuitive™. A robotic-assisted endoluminal platform for minimally invasive peripheral lung biopsy," 2021, Accessed: Feb. 22, 2021. [Online]. Available: https://www.intuitive.com/en-us/products-and-services/ion

[96] E. E. Folch *et al.*, "A prospective, multi-center evaluation of the clinical utility of the ion endoluminal system-experience using a robotic-assisted bronchoscope system with shape-sensing technology," in *A110. Advances in Interventional Pulmonology*, New York, NA, USA: American Thoracic Society, 2020, pp. A2719–A2719.

[97] A. Agrawal, D. K. Hogarth, and S. Murgu, "Robotic bronchoscopy for pulmonary lesions: A review of existing technologies and clinical data," *J. Thorac. Dis.*, vol. 12, no. 6, 2020, Art. no. 3279.

[98] Virtuoso Surgical Inc., "Virtuoso surgical," 2020, Accessed: Sep. 9, 2021. [Online]. Available: https://virtuososurgical.net

[99] Medrobotics Corporation, "Flex robotic system: Expanding the reach of surgery," 2021, Accessed: Feb. 22, 2021. [Online]. Available: https://medrobotics.com/gateway/flex-system-int
[100] S. Mattheis *et al.*, "Flex robotic system in transoral robotic surgery: The first 40 patients," *Head Neck*, vol. 39, no. 3, pp. 471–475, 2017.
[101] M. Remacle, V. M. N. Prasad, G. Lawson, L. Plisson, V. Bachy, and S. Van der Vorst, "Transoral robotic surgery (TORS) with the medrobotics flex^{TM} System: First surgical application on humans," *Eur. Arch. Oto-Rhino-Laryngol.*, vol. 272, no. 6, pp. 1451–1455, 2015.
[102] N. Sethi *et al.*, "Transoral robotic surgery using the medrobotic flex system: The adelaide experience," *J. Robot. Surg.*, vol. 14, no. 1, pp. 109–113, 2020.
[103] I. D. Walker *et al.*, "Continuum robot arms inspired by cephalopods," in *Proc. Unmanned Ground Veh. Technol. VII*, 2005, pp. 303–314.
[104] M. Runciman, A. Darzi, and G. P. Mylonas, "Soft robotics in minimally invasive surgery," *Soft Robot,* vol. 6, no. 4, pp. 423–443, 2019.
[105] M. Cianchetti, C. Laschi, A. Menciassi, and P. Dario, "Biomedical applications of soft robotics," *Nat. Rev. Mater.*, vol. 3, no. 6, pp. 143–153, 2018.
[106] M. Manti, V. Cacucciolo, and M. Cianchetti, "Stiffening in soft robotics: A review of the state of the art," *IEEE Robot. Autom. Mag.*, vol. 23, no. 3, pp. 93–106, Sep. 2016.
[107] Y. Lee, W. J. Song, and J.-Y. Sun, "Hydrogel soft robotics," *Mater. Today Phys.*, vol. 15, 2020, Art. no. 100258. [Online]. Available: https://doi.org/10.1016/j.mtphys.2020.100258
[108] E. Palleau, D. Morales, M. D. Dickey, and O. D. Velev, "Reversible patterning and actuation of hydrogels by electrically assisted ionoprinting," *Nat. Commun.*, vol. 4, no. 1, pp. 1–7, 2013.
[109] J. Zheng *et al.*, "Mimosa inspired bilayer hydrogel actuator functioning in multi-environments," *J. Mater. Chem. C*, vol. 6, no. 6, pp. 1320–1327, 2018.
[110] R. Prewitt, V. Bochkarev, C. L. McBride, S. Kinney, and D. Oleynikov, "The patterns and costs of the da vinci robotic surgery system in a large academic institution," *J. Robot. Surg.*, vol. 2, no. 1, pp. 17–20, 2008.
[111] C. Culmone, P. W. J. Henselmans, R. I. B. van Starkenburg, and P. Breedveld, "Exploring non-assembly 3D printing for novel compliant surgical devices," *PLoS One*, vol. 15, no. 5, 2020, Art. no. e0232952.
[112] T. K. Morimoto and A. M. Okamura, "Design of 3-D printed concentric tube robots," *IEEE Trans. Robot.*, vol. 32, no. 6, pp. 1419–1430, Dec. 2016, doi: 10.1109/TRO.2016.2602368.
[113] K. Oliver-Butler, Z. H. Epps, and D. C. Rucker, "Concentric agonist-antagonist robots for minimally invasive surgeries," in *Proc. SPIE 10135, Med. Imag. 2017: Image-Guided Procedures, Robotic Interv., Model.*, 2017, Art. no. 1013511, doi: 10.1117/12.2255549.
[114] R. J. Webster, A. M. Okamura, and N. J. Cowan, "Toward active cannulas: Miniature snake-like surgical robots," in *Proc. IEEE/RSJ Int. Conf. Intell. robots Syst.*, 2006, pp. 2857–2863.

Costanza Culmone studied from the University of Pisa, Italy, where she received the M.Sc. degree in biomedical engineering in 2016. She is currently working toward the Ph.D. degree in biomechanics with the Delft University of Technology, Delft, The Netherlands. In 2015, she was an intern with the Minimally Invasive Surgery and Interventional Techniques (MISIT) Group, Delft University of Technology, where she worked on a variable stiffness needle for percutaneous interventions. Her master thesis focused on cardiovascular interventions and was a joint collaboration between the BioRobotic Institute of Scuola Superiore Sant'Anna (SSSA) and the BITE Group, Delft University of Technology. Her research interests include surgical instruments with a focus on additively manufactured steerable devices and shape memory systems.

Fatih S. Yikilmaz was born in Gouda, The Netherlands, in 1996. He received the B.Sc. and M.Sc. degrees in mechanical engineering from the Delft University of Technology, Delft, The Netherlands, in 2017 and 2021, respectively. He is an Intern with the Department of Biomechanical Engineering. His research interests include follow-the-leader systems and mechanical systems for surgical endoscopy.

Fabian Trauzettel born in Germany, he has spent most of his life in Ireland, graduating with a bachelor's degree in biomedical engineering from the Cork Institute of Technology, Ireland, in 2016, where his graduation project focused on the adaptation of FDM 3D printing to print with a liquid PVC plastisol. He is a Biomedical / Mechanical Engineer working as an early-stage Researcher of the ATLAS Marie Curie European Joint Doctorate School between the BITE group with the Delft University of Technology, Delft, The Netherlands, and the RAS Group at KU Leuven, Leuven, Belgium. Having gained a taste for research work, he began a research master's at University College Cork. The subject of his thesis was the modeling and experimental validation of a steerable, electromagnetically tracked catheter for bronchoscopy in the peripheral airways, and largely took place at the institute for image guided surgery (IHU) in Strasbourg. During this time, he came into direct contact with research in the fields of natural orifice surgery, intraluminal surgery, hyperspectral imaging, computer vision, laparoscopic surgery, endovascular interventions, medical simulation, and surgical training. He now works on the design of multi-steerable flexible medical instruments, with a focus on 3D printing and minimal-assembly designs.

Paul Breedveld studied mechanical engineering with the Delft University of Technology (TU Delft), Delft, The Netherlands, where he received the M.Sc. (with Hons.) and Ph.D. (with Hons.) degrees in 1991 and 1996. Extending his experience in space robotics to the medical field, he continued his research with the design of innovative medical devices inspired by smart biological solutions, sponsored by grants from the Royal Netherlands Academy of Arts and Sciences. His research was rewarded in 2012 with a prestigious Dutch VICI grant on the development of advanced snake-like instrumentation for endo-nasal skull base surgery, and in 2013 with an Antoni van Leeuwenhoek distinguished professorship at TU Delft. In 2014, he was one of the founders of the PainLess Foundation: a Dutch initiative to find solutions for chronic and incurable pain, and in 2019, he became one of the chairs of Dutch Soft Robotics, a Dutch national research program on soft robotic systems. Being principal investigator in a number of national and EU research programs, he is currently the Chair of the section Minimally Invasive Surgery and Bio-Inspired Technology, TU Delft and the Director of the Graduate School of the faculty 3mE.